DOI: 10.26599/FSHW.2026.9251288

Y.Hu et al. / Food Science and Human Wellness 17 (2028)

Contents lists available at SciOpen

Food Science and Human Wellness

journal homepage: https://www.sciopen.com/journal/2097-0765

China Food Publishing Co.

Co-culture of *Acetobacter pasteurianus* and *Lactobacillus plantarum* enhances biofilm formation and improves vinegar characteristics

Yong Hu[1,2,3#], Haiyin Chen[1#], Chunling Chen[1], Hanjian Zhu[1], Tingyu Zhou[1], Chao Wang[1], Wei Li[1], Ning Xu[1], Mengzhou Zhou[1*]

[1]*Key Laboratory of Fermentation Engineering (Ministry of Education), Hubei Key Laboratory of Industrial Microbiology, National "111" Center for Cellular Regulation and Molecular Pharmaceutics, Hubei Research Center of Food Fermentation Engineering and Technology, Cooperative Innovation Center of Industrial Fermentation (Ministry of Education & Hubei Province), Hubei University of Technology, Wuhan, 430068, Hubei, People's Republic of China.*

[2]*Suizhou February Wind Food Co., Ltd., 431518, Suizhou, China.*

[3]*Hubei Xizhiyuan Bioengineering Co., Ltd, 445099, Enshi, China.*

ABSTRACT: Acetic acid bacteria and lactic acid bacteria are core microbial components in traditional Chinese vinegar brewing, where biofilm-associated microflora form unique and stress-resilient consortia. This study explored bacterial adaptive responses and biofilm development in bicultures of *Acetobacter pasteurianus* with individual *Lactobacillus* strains. Across all bi-cultures, *A. pasteurianus* exhibited a competitive dominance over *Lactobacillus* strains. Notably, co-cultivation of *A. pasteurianus* with *L. plantarum* markedly promoted biofilm formation, independent of autoinducer-2 signaling. Transcriptomic and metabolomic analyses revealed that both strains employed effective acid-resistance strategies. However, *A. pasteurianus* prioritized energy generation and intracellular redox balance, whereas *L. plantarum* enhanced biosynthesis of cellular building blocks. Complementary pathways, including those involved in lactic acid, sorbose/sorbitol, and galactose/galactitol metabolism, facilitated interspecific mutual adaptation. These regulations, together with increased production/export of lipopolysaccharides, lipoproteins, organic acids, amino acids and nucleotides, as well as the activated quorum sensing and biofilm pathways in *A. pasteurianus*, collectively reinforced the co-cultured biofilm development. Further, *A. pasteurianus-L. plantarum* co-fermentation significantly improved acid production and antioxidant activity of vinegar. This study provides insights into the regulatory mechanisms for the dominance of *A. pasteurianus* over *L. plantarum* and the enhanced biofilm formation in their co-culture, offering implications for optimizing their application in vinegar fermentations.

Keywords: *Acetobacter pasteurianus*; *Lactobacillus*; Biofilm; Multi-omics; Vinegar fermentation

1. Introduction

Biofilm are structured communities of bacteria embedded within a self-produced extracellular matrix composed of proteins, extracellular polysaccharides (EPS), lipids, bacteriocins, low-molecular-mass solutes, and nucleic acids released from lysed cells[1]. Following the initial attachment of planktonic cells to a solid surface, EPS-mediated physical adhesion initiates biofilm development, a process tightly regulated by quorum

[#]Authors contribute equally to the study.
***Corresponding author**
zmzkelvin@hbut.edu.cn (M.Z. Zhou)

Received 14 February 2026
Received in revised from 31 March 2026
Accepted 11 May 2026

sensing (QS), a cell-to-cell communication mechanism that monitors population density to coordinate gene expression[2]. QS regulates various physiological processes, including virulence factor secretion, sporulation, and DNA uptake competence[3]. Nevertheless, biofilm formation is influenced by multiple factors beyond QS. For example, hydrolases, pantothenate kinase, non-coding small RNAs, and metabolic pathways such as bacterial chemotaxis, porphyrin–chlorophyll metabolism, and sulfur metabolism have been implicated in modulating biofilm formation in *Salmonella enteritidis* and *Streptococcus mutans*[4-5].

While biofilms preferentially form as bacteria grow on solid surfaces, their development is often driven by defense against environmental stresses, colonization of favorable niches, and the collective benefits of community living. Indeed, this communal lifestyle represents one of the most successful survival strategies in diverse environments[6-7]. Interspecies microbial interactions often promote biofilm formation and stability, improving the coexistence of the community. For instance, *Enterococcus* biofilms can facilitate the attachment of *Campylobacter jejuni*[8]. Compared to monospecies biofilms, multispecies biofilms are generally more robust and resilient, contributing to microbial persistence under harsh conditions, and thus can be important for microbial vitality in microecological system[9]. Since biofilm dynamics can promote the dissemination of pathogens and spoilage microorganisms by providing a stable and protective niche, it is of particular importance to develop strategies that reduce biofilm resistance or effectively control its formation.

Traditional Chinese vinegar are typically produced in static and open systems, starting from solid biomaterials and proceeding through complex interactions between microbial communities and their environments. During fermentation, extensive biochemical transformations occur, generating diverse compound profiles that define the flavor and functional characteristics of the final products. While the nutrient competition and stress adaptation drive microbial antagonism, mutualistic interactions foster symbiosis within the community[10-11]. Due to the hydrophobic nature of raw materials and low-shear static conditions, the vinegar fermentation environment favors microbial adhesion and biofilm formation, which enhance microbial persistence and functional performance during fermentation.

Acetic acid bacteria (AAB) and lactic acid bacteria (LAB) constitute the dominant bacteria in traditional Chinese vinegar fermentation[12-13]. AAB are the key functional bacteria that oxidize ethanol to acetic acid, creating a strong acidic environment stressful to other microbes. In a solid-state fermentation of cereal vinegar with *Lactobacillus helveticus* CGMCC 12062 and *Acetobacter pasteurianus* CGMCC 3089[14], carbohydrate, amino acid, purine, and pyrimidine metabolism were downregulated in *L. helveticus* but upregulated in *A. pasteurianus* compared with mono-cultures. LAB biofilms have been well characterized for their enhanced stress resistance[15], and increasing evidence has revealed complex regulatory mechanisms underlying biofilm formation [16-17]. For example, 1,051 genes involved in pyrimidine and glycerol metabolism, amino acid biosynthesis, extracellular enzyme production, and stress responses were differentially expressed between planktonic and biofilm cells of *Lactobacillus plantarum* J26[18]. However, the mechanisms underlying biofilm formation in AAB remain largely unclear, although lactic acid has been reported to induce biofilm formation in *A. pasteurianus*[19]. LAB are capable of forming mixed-species

biofilms with other functional microbes that assist in fermentation processes. For instance, *L. plantarum* ML11-11 and *Saccharomyces cerevisiae* can establish direct cell-cell contact to form a robust mixed-species biofilm under static co-culture conditions[20-21]. The complementary properties of these two microorganisms enhance biofilm formation: LAB secrete enzymes that produce low-molecular-weight nutrients for yeast, while yeast catalase protects LAB from oxidative stress[19]. The formation and regulation of mixed biofilms between AAB and LAB during vinegar fermentation remain largely unknown.

Furthermore, co-fermentation with *L. plantarum* can accelerate fermentation kinetics through metabolic complementation, balance substrate consumption via metabolite cross-feeding, promote the synthesis of characteristic flavor compounds, and reduce the accumulation of off-flavor substances[22]. Biofilm formation can also change organic acid composition such as malic acid, thus influencing fermented food quality[23]. Previous studies confirmed that adding *L. plantarum* during fruit vinegar fermentation significantly improves flavor and taste[24-27]. Lactic acid produced by *L. plantarum* not only improves vinegar quality directly but can also be converted into acetoin by *A. pasteurianus*, jointly enhancing the overall quality of vinegar[28]. The regulation of mixed biofilms may reshape microbial metabolism, alter metabolite profiles, and ultimately affect vinegar flavor and quality. Elucidating such mechanisms will help reveal microbial community behavior and provide a basis for optimizing vinegar fermentation.

In this study, *L. plantarum*, *L. casei*, and *L. fermentum* were compared for their ability to promote mixed-species biofilm formation with *A. pasteurianus* 141. The role of autoinducer-2 (AI-2), a QS signaling molecule, in biofilm formation was specifically investigated. Transcriptomic and metabolomic analyses were performed to compare gene expression and metabolite profiles between biofilm cells of *L. plantarum* and *A. pasteurianus* in co-culture and monoculture. In addition, the effects of *L. plantarum*-*A. pasteurianus* co-fermentation on vinegar characteristics were evaluated. This study provides new insights into the regulatory mechanisms of enhanced biofilm formation in the co-culture of *L. plantarum* and *A. pasteurianus*, as well as a practical basis for improving vinegar production in the fermentation industry.

2. Materials and methods

2.1 Bacterial strains

L. plantarum, *L. casei* and *L. fermentum* were cultured in de Man–Rogosa–Sharpe (MRS) medium at 37℃. *A. pasteurianus* 141 was grown in GY medium containing 2% (w/v) glucose and 2% (w/v) yeast extract at 30℃. *Vibrio harveyi* BB170 was cultivated in autoinducer bioassay (AB) medium at 30℃[29]. The bacterial concentration was determined at an optical density of 600 nm (OD_{600}) using a spectrophotometer (UV1601, Ruili, China).

2.2 Biofilm quantification

Lactobacillus strains and *A. pasteurianus* were precultured for 24 h and then diluted in their respective media (ethanol was added when needed) to approximately 1×10^7 colony-forming units per milliliter (CFU/mL). For mono-cultures, 200 μL bacterial suspension was added per well in a 96-well plate. For

co-cultures, 100 μL *A. pasteurianus* and 100 μL *Lactobacillus* strain were combined per well, following a previously described method[30]. The cultures were were statically cultured at 30 ℃. At designated time points (24 h, 48 h, and 72 h), the supernatants were collected to measure planktonic cell density at 600 nm. The wells were then gently washed three times with 200 μL of sterile normal saline to remove non-adherent cells. Biofilm biomass was quantified using the crystal violet staining assay, and absorbance was measured at 590 nm[31].

2.3 Cells counting

Bacterial suspensions were collected, serially diluted up to 10^7-fold with sterile normal saline, and spread onto agar plates. Plates were incubated at 30℃ for enumeration of planktonic cells. After rinsing the wells with normal saline, a sterile cotton swab was used to collect the attached biofilm cells, which were then transferred into sterile tubes containing 200 μL of normal saline. The tubes were vortexed for 30 s to disperse the cells. The suspensions were diluted and plated on MRS agar for CFU determination. Colonies with milky-white and dark-yellow morphology were identified as *Lactobacillus* strains and *A. pasteurianus*, respectively.

2.4 Microscopic observation

Biofilms were formed on glass slides placed in 6-well polystyrene microtiter plates. After incubation for 72 h, the slides were rinsed three times with normal saline. Gram stained biofilms were observed under a light microscope equipped with a 100× oil immersion objective (Nikon MM600, Tokyo, Japan).

For **scanning electron microscopy (SEM)** analysis, samples were fixed in 2.5% (w/v) glutaraldehyde at room temperature for 4 h, rinsed three times with phosphate buffer (15 min each), and dehydrated through a graded ethanol series (50%, 60%, 70%, 80%, 90%, 95%, and 100%, 10 min each). The samples were then critical-point dried with CO_2, mounted on aluminum stubs using carbon adhesive tabs, and sputter-coated with silver and palladium. Imaging was performed with a SEM (**JEOL JSM-6390LV,** Tokyo, Japan) at 5 kV.

For viability assessment, slides were stained according to the manufacturer's instructions using the **Live/Dead™ BacLight™ Bacterial Viability Kit** (Thermo Fisher Scientific, USA). SYTO9, a green fluorescent nucleic acid dye, stains live bacteria with intact membranes, while propidium iodide (PI), a red fluorescent nucleic acid dye, stains dead or membrane-compromised bacteria. Stained slides were examined using a **confocal laser scanning microscope (CLSM; Leica SP8, Leica, Germany)** equipped with a 63× oil immersion objective. Excitation wavelengths of 488 nm and 552 nm were used to visualize SYTO9 and PI fluorescence, respectively[32].

2.5 Detection of AI-2 activity

AI-2 activity was measured using *V. harveyi* BB170 as the reporter strain, following the method in a previous report[33]. Briefly, overnight culture of BB170 was diluted 1:5000 in fresh AB medium to prepare the assay solution. Cell-free supernatant from BB170 and AB medium alone were used as positive and

negative controls, respectively. Sample cell-free supernatants were mixed with the assay solution at a 1:100 (v/v) ratio and incubated at 30℃ with gentle shaking. Fluorescence was measured using a multilabel plate reader (Varioskan LUX, Thermo Scientific, USA), and relative fluorescence intensity was calculated with reference to the minimum fluorescence of the negative control. Artificially synthesized AI-2 (stored in the laboratory) was added to the medium at a final concentration of 60 μM. D-galactose (Shanghai Pharmaceutical Group Co., Ltd., Shanghai, China) was used at a final concentration of 0.2 M[34].

2.6 Metabolomic measurement

After cultivation with 6% initial ethanol for 72 h, biofilm cells were collected into a 2 mL centrifuge tube, washed 3 times with distilled water, and vortexed together with 100 mg glass bead and 1000 μL 50% methanol water (4℃) for 30 s. After freezing in liquid nitrogen for 5 min, the sample was ground twice at 55 Hz for 2 min in a grinder (MB-96, Zhejiang Meibi Experiment Equipment Co., Ltd., Zhejiang, China). The mixture was centrifuged for 10 min (12,000 rpm and 4℃), and the supernatant was dried. The powder was redissolved with 2-amino-3-(2-chloro-phenyl)-propionic acid (4 ppm) solution prepared with 50% methanol water, and filtered through 0.22 μm membrane.

Liquid chromatography (Vanquish UHPLC System (Thermo Fisher Scientific, USA) - mass spectrometer (LTQ-OrbiTrap 120, Thermo Fisher Scientific, USA) (LC-MS) detection was performed to identify metabolites in Shanghai Personalbio Technology Co., Ltd (Shanghai, China). Chromatography was carried out with an ACQUITY UPLC® HSS T3 (150 × 2.1 mm, 1.8 μm) (Waters, Milford, MA, USA). The column was maintained at 40℃. The flow rate and injection volume were set at 0.25 mL/min and 2 μL, respectively. For LC-ESI (+)-MS, the mobile phases consisted of (A) 0.1% formic acid in acetonitrile (v/v) and (B) 0.1% formic acid. Separation was conducted as follows: 0~1 min, 2% A; 1~9 min, 2%~50% A; 9~12 min, 50%~98% A; 12~13.5 min, 98% A; 13.5~14 min, 98%~2% A; 14~20 min, 2% A. For LC-ESI (-)-MS, acetonitrile (C) and ammonium formate (5mM) (D) were used as follows: 0~1 min, 2% C; 1~9 min, 2%~50% C; 9~12 min, 50%~98% C; 12~13.5 min, 98% C; 13.5~14 min, 98%~2% C; 14~17 min, 2% C. The following parameters were used: sheath gas pressure, 30 arb; aux gas flow, 10 arb; spray voltage, 3.50 kV and -2.50 kV for ESI(+) and ESI(-), respectively; capillary temperature, 325℃; MS1 range, m/z 100-1000; MS1 resolving power, 60,000 FWHM; number of data dependant scans per cycle, 4; MS/MS resolving power, 15,000 FWHM; normalized collision energy, 30%; dynamic exclusion time, automatic.

2.7 Transcriptomic sequencing

Biofilm cells were gently washed 3 times with sterile PBS (pH 7.2) prepared with DEPC water. Then, 1 mL of PBS-DEPC was added, and suspended cells were transferred to a centrifuge tube. After centrifugation at 4℃ for 10 min, PBS was discarded, and precipitated cells were quickly frozen in liquid nitrogen.

Total RNA was extracted using TRIzol Reagent /RNeasy Mini Kit (Invitrogen, CA). The genomic DNA was digested using DNase I (TaKara, Kyoto, Japan). RNA quality was determined using an Agilent 2100 bioanalyzer (Agilent, Palo Alto) and quantified using an ND-2000 (NanoDrop Technologies, Thermo

Electron Corporation, NY). The rRNA was depleted from total RNA using Pan-ribo-pools Kit (Beijing Foreverstar Biotech Co., Ltd., Beijing, China). One microgram RNA was used for library preparation. Briefly, RNA was fragmented and the first strand cDNA was synthesized using ProtoScript II Reverse Transcriptase (Invitrogen, CA) with random hexamers. The double-strand cDNA was synthesized using the SuperScrip Double-Strand cDNA Synthesis kit (Invitrogen, CA). The DNA was purified and treated with End Prep Enzyme Mix (New England BioLabs, MA, USA) to repair both ends and add a dA-tailing, followed by a T-A ligation to add adaptors to the ends. Adaptor-ligated DNA fragments of about 400 bp were recovered. The dUTP-marked second strand was digested with Uracil-Specific Excision Reagent enzyme (New England BioLabs, MA, USA). The amplified DNA products of each sample were cleaned up, validated using an Qsep100 (Bioptic, Taiwan, China), and quantified by Qubit3.0 Fluorometer (Invitrogen, Carlsbad, CA, USA). Sequencing was performed on Illumina Hiseq 2500 platform (Suzhou Genewiz Biotechnology Co., Ltd., Suzhou, China).

2.8 Data processing and analysis

In metabolomics, raw data were converted using MSConvert in the ProteoWizard R package (v3.0.8789) and processed with XCMS[35]. Metabolite identification was based on accurate mass (< 30 ppm) and MS/MS data using the HMDB (http://www.hmdb.ca)[36], MassBank (http://www.massbank.jp)[37], LipidMaps (http://www.lipidmaps.org)[38], mzCloud (https://www.mzcloud.org)[39] and KEGG databases (Kyoto Encyclopedia of Genes and Genomes) (http://www.genome.jp/kegg/)[40]. After normalization using quality control-based random forest correction (QC-RFSC)[41], ion peaks with relative standard deviations (RSDs) less than 30% in quality control samples were retained. Metabolites with $p \leq 0.05$ and $|\log_2 \text{fold-change}| \geq 1$ were considered significantly differential.

In **transcriptomics**, raw reads were trimmed using **Cutadapt** (v1.9.1)[42] to remove adapters, sequences shorter than 20 bp, low-quality bases ($Q \leq 20$) at the 5′ or 3′ ends, and reads containing N. Clean reads were aligned to reference genomes using **Hisat2** (v2.0.1)[43]. The genome of *A. pasteurianus* 141 was obtained from a previous study[44], and the genome of *L. plantarum* is available in GenBank (CP020816.1). Gene expression levels were quantified as transcripts per million (TPM) using **HTSeq** (v0.6.1)[45]. Genes with false discovery rate (FDR)-adjusted $p \leq 0.05$ and $|\log_2 \text{fold-change}| \geq 1$ were defined as differentially expressed genes (DEGs).

Metabolomic pathways were annotated using the KEGG database via **MetaboAnalyst 5.0** (http://www.metaboanalyst.ca/)[46]. KEGG enrichment of DEGs was analyzed online (https://www.omicshare.com/), and **Gene Set Enrichment Analysis (GSEA)** was performed referencing KEGG pathways (https://cloud.oebiotech.cn/task/)[47]. **Multivariate statistical analyses** included principal component analysis (PCA) using R 4.4.1 and two-way orthogonal partial least squares discriminant analysis (O_2PLS-DA) using SIMCA 14.1 (32-bit) with thresholds $P < 0.05$ and VIP > 1. Linear discriminant analysis effect size (LEfSe, LDA > 2.5) and random forest analyses were conducted online (https://bioincloud.tech/task-meta). Visualization of data including heat maps, volcano plots, venn diagrams,

and hierarchical clustering analysis (HCA) based on Euclidean distance were created online (https://cloud.metware.cn). For network analysis, metabolite-associated proteins were retrieved using the KEGGREST package in R. Protein–protein interactions were obtained from STRING (https://cn.string-db.org/) with default parameters. Networks were constructed using NetworkAnalyst 3.0 (https://www.networkanalyst.ca)[48] and visualized using[49].

2.9 Quantitative reverse transcription-polymerase chain reaction (qRT-PCR)

After synthesis of cDNA with ProtoScript II Reverse Transcriptase (Invitrogen, CA) and random hexamers, the expressions of *pfs* (encoding adenosylhomocysteine nucleosidase), *luxS* (S-ribosylhomocysteinase) and *luxR* (receptor of AI-2) were verified on an ABI prism 7300 Real-Time PCR system (Applied Biosystem, CA, USA) using the ChamQ SYBR Color qPCR Master Mix (Nanjing Nuoweizan Biotechnology Co., Ltd, Nanjing, China). *gyrB* was used as the internal control. The primers were listed in Table S1.

2.10 Manipulation of solid-state vinegar

Glutinous rice (10 kg) was soaked for 10 h, drained, and then cooked for 20 min. The cooked glutinous rice was inoculated with 2.0 mL of α-amylase (activity >80,000 U/mL, Jiangsu Boli Biological Products Co., Ltd., Wuxi, China) and incubated at a temperature above 85℃ for 30 min. The mixture was then turned over to cool down to 60℃, followed by the addition of 4 mL of glucoamylase (activity >200,000 U/mL, Jiangsu Boli Biological Products Co., Ltd., Wuxi, China), and the incubation was continued at 60℃ for 0.5 h. Subsequently, the mixture was transferred into a pottery pot and allowed to cool naturally to room temperature (approximately 28℃). Overnight-cultivated *S. cerevisiae* was thoroughly mixed with the mash to initiate alcoholic fermentation for 2 days. For acetic acid fermentation (AAF), bran (12 kg), rice husk (14 kg) and bacterial seed suspension (1.2 L) were added to the mash and mixed well. For preparation of bacterial seeds, the cultures were centrifuged and resuspended in sterile water to achieve a considerable viable bacteria count (1×10^9 CFU/mL) for both the single *A. pasteurianus* seed suspension and the mixed seed suspension of *L. plantarum* and *A. pasteurianus*. *L. plantarum* and *A. pasteurianus* were present at an equal ratio in their mixture. The mash was turned over daily during the fermentation. After 18 days of fermentation, the pottery pot was sealed, and the fermentation was continued for an additional 20 days. Finally, 45 kg of water was added to the fermented mash for vinegar leaching.

2.11 Determination of organic acids, total polyphenols (TP) and total flavonoids (TF) and antioxidant activity

Vinegar samples were centrifuged at 7000 rpm for 10 min, and the resulting supernatants were filtered through a 0.22 μm membrane filter prior to subsequent determinations. The total acid content was quantified as acetic acid equivalents in accordance with the national standard GB/T 5009.41-2003[50]. Organic acid profiles were analyzed by HPLC (Waters 1515, Waters Co., Milford, MA, USA) equipped with a YMC-Pack

ODS-AM C_{18} column (250 mm × 4.6 mm, 5 μm; YMC Co., Tokyo, Japan). The analytical procedure was performed as described previously[51].

Gallic acid and rutin were used as the standard reference compounds for the preparation of calibration curves for the determination of TP and TF , with distilled water serving as the blank control. The antioxidant activity of the samples was evaluated via 2,2-diphenyl-1-picrylhydrazyl (DPPH) radical scavenging and ABTS radical cation scavenging assays. All all operations were conducted following the method reported previously[51].

2.12 Statistical analysis

All experiments were performed in triplicate. An analysis of variance (ANOVA) was performed to determine statistical difference (SD). The means were compared by applying Duncan's multiple-range test using SPSS software (version 26) (SPSS Inc., Chicago, IL, USA). The SD was considered to be significant at the $*P < 0.05$, $** P < 0.01$ and $*** P < 0.001$.

2.13 Data availability

Raw transcriptomic data have been deposited in the Genome Sequence Archive in China National Center for Bioinformation-National Genomics Data Center (CNCB-NGDC) (GSA: CRA031924) at https://ngdc.cncb.ac.cn/gsa.

3. Results and discussion

3.1 Biofilm formation in cultures of A. pasteurianus and Lactobacillus strains

In cultures without ethanol, *L. plantarum* and *L. casei* exhibited higher planktonic biomass than *L. fermentum* and *A. pasteurianus* (Fig. 1A). Co-cultivation of *A. pasteurianus* with individual *Lactobacillus* strains significantly increased the cell density (Fig. 1A). Under 6% initial ethanol, the planktonic biomass of all cultures were suppressed, but it was obviously higher in co-culture of *A. pasteurianus and L. plantarum* which even reached the level without ethanol at 48-72 h (Fig. 1A). Cell counting at 72 h displayed a comparable pattern (Fig. 1B). From the cell counting, the increase of total cell number in dual bacterial co-cultures was largely due to the increase of *A. pasteurianus*, where *Lactobacillus* strains suffered from some inhibition compared with the mono-cultures (Fig. 1B).

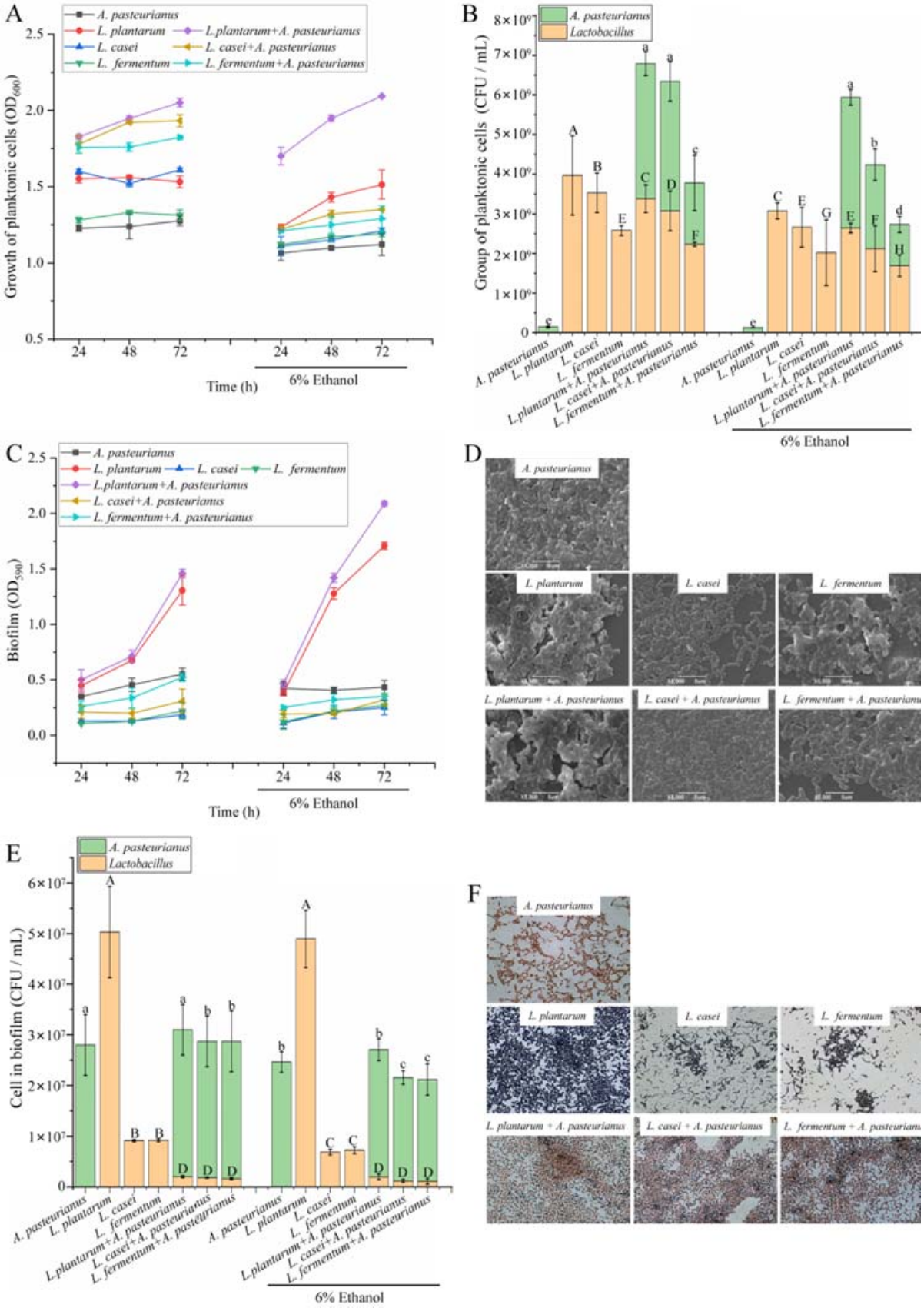


Fig. 1 Bacterial growth and biofilm formation in mono- and bi-cultures. (A) The planktonic cell growth in cultures. (B) The viable cell counting of *Lactobacillus* strains and *A. pasteurianus* recovered from 72 h planktonic cultures. (C) The biofilm formed in cultures. (D) SEM of 72 h biofilms in cultures with 6% initial ethanol. (E) The viable cell counting of *Lactobacillus* strains and *A. pasteurianus* recovered from 72 h biofilms. (F) Gram's stain of *Lactobacillus* strains and *A. pasteurianus* embedded in 72 h biofilms cultured with 6% initial ethanol. In B and E, different lowercase letters represent the significant difference of *A. pasteurianus* numbers in cultures ($p < 0.05$), and different capital letters represent significant differences of *Lactobacillus* numbers in cultures ($p < 0.05$).

L. plantarum produced higher amount of biofilm than other strains in mono-cultures at 48-72 h, whether ethanol was present or not (Fig. 1C). Its co-cultivation with *A. pasteurianus* further increased biofilm formation, particularly in the presence of ethanol (Fig. 1C). In contrast, co-cultures of *A. pasteurianus* with *L. casei* or *L. fermentum* did not produce more biofilm. These observations were consistent with the SEM examination (Fig. 1D): thick and rough biofilms accumulated on glass coverslips in the *L. plantarum* mono-culture and its co-culture with *A. pasteurianus*, whereas thin and smooth layers were observed in the other cultures. Similar enhancement of biofilm formation was reported in the bi-culture of *Pseudomonas fluorescens* and *Staphylococcus aureus*[52]. In cell counting at 72 h, *A. pasteurianus* and especially *L. plantarum* produced more biofilm-associated cells than the other two *Lactobacillus* strains in mono-cultures (Fig. 1E). However, their numbers had less discrepancy in co-cultured biofilms, where *A. pasteurianus* accounted for 93.5-94.4% of total cells (Fig. 1E), as supported by Gram staining (Fig. 1F). These proportions were much higher than those observed in co-cultured planktonic cells (42.1-51.6%), suggesting that strains were differentially regulated depending on their ecological niches. The *A. pasteurianus* exhibited robust tolerance to acetic acid through multiple adaptive mechanisms[53], whereas growth of *Lactobacillus* strains was strongly inhibited by acetic acid[54]. Moreover, *A. pasteurianus* has evolved a metabolic strategy that prioritizes speed over efficiency[55], preferring ethanol as the carbon source for energy generation[56]. Thus, the metabolites may play central roles on establishment of a commensal relationship conferring a metabolic advantage to *A. pasteurianus* over the *Lactobacillus* strains[14,57]. The results implied that specific metabolic regulation can occur in the interplay between *L. plantarum* and *A. pasteurianus for the* biofilm enhancement.

3.2 Independence of enhancement of co-cultured biofilms on excess AI-2 production

Bacterial communication usually relies on the secretion and sensing of AIs as signaling molecules. AI-2 plays a pivotal role in regulating growth and biofilm formation in both Gram-negative and Gram-positive bacteria, including LAB[58-59]. The biological activity of AI-2 was verified using *V. harveyi* BB170 as an indicator strain (Fig. S1). Then, the effect of AI-2 on cultures was assessed at 6% ethanol concentration. Supplementation with AI-2 significantly promoted only the planktonic biomass of mono-cultured *Lactobacillus* strains (Fig. 2A), but it enhanced biofilm formation in all *Lactobacillus*-contained cultures (Fig. 2B). To confirm the positive role of AI-2 in biofilm development, D-galactose was added as an AI-2 inhibitor[34]. D-galactose exhibited no effect on planktonic biomass in various cultures (Fig. 2C); however, it significantly reduced biofilm formation in cultures (Fig. 2D). The results revealed that the presence of AI-2 significantly can increase *Lactobacillus* resistance to ethanol stress and enhance their mono- and co-cultures biofilm formation.

In mono-cultures, *L. plantarum* naturally exhibited the highest AI-2 activity, followed by *L. casei*, whereas *L. fermentum* and *A. pasteurianus* showed almost no detectable AI-2 activity (Fig. 2E), confirming that *Lactobacillus* strains differ in their AI-2 signaling intensities[60]. However, AI-2 production was not further elevated in co-cultures (Fig. 2E). This result suggested that factors other than AI-2 are responsible for the enhanced biofilm formation in the co-culture of *L. plantarum* and *A. pasteurianus*[61-62].

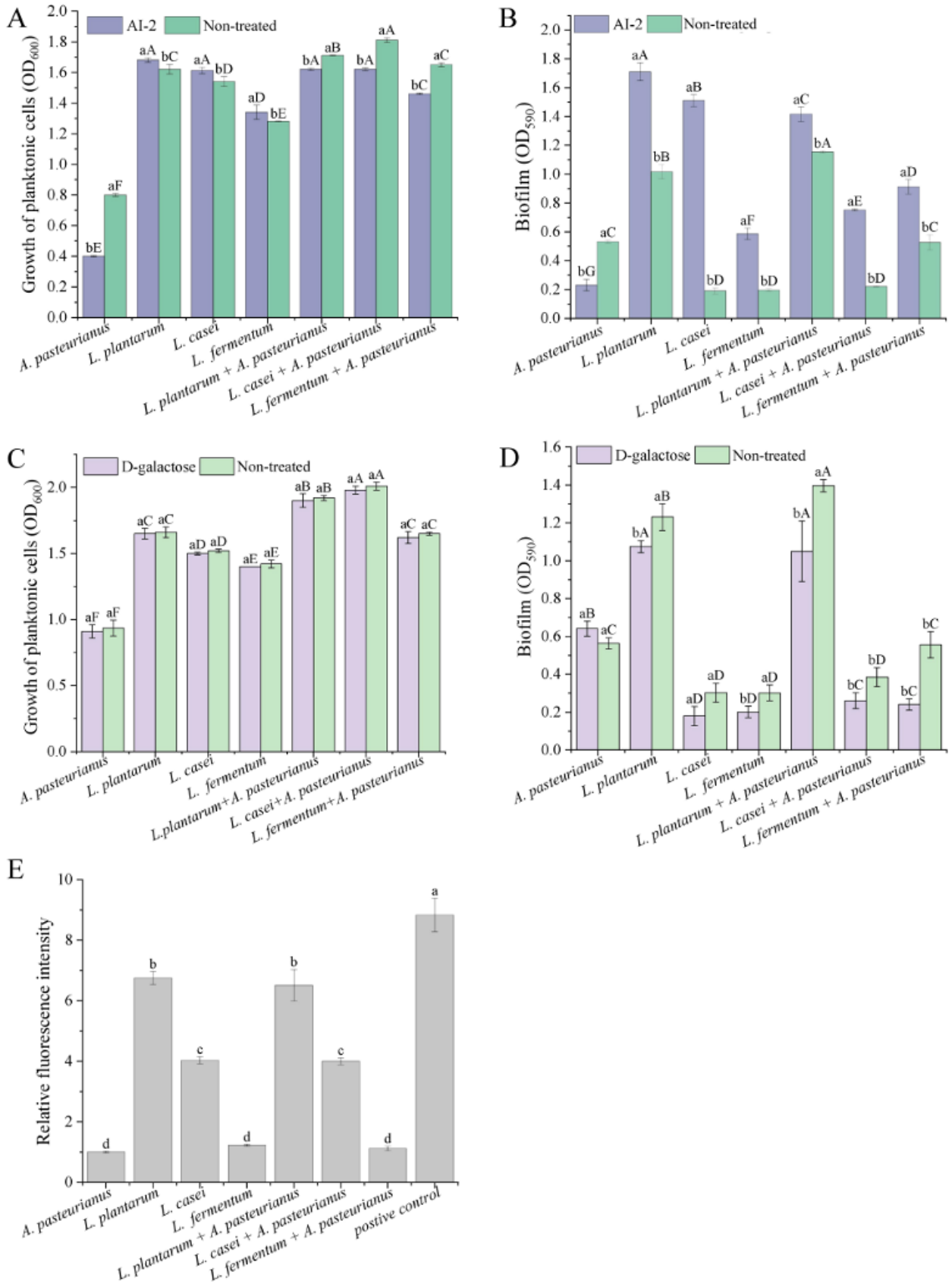


Fig. 2 Effect of AI-2 on the bacterial growth and biofilm formation at 6% ethanol. (A) Effect of AI-2 on planktonic cell growth. (B) Effect of AI-2 on biofilm formation. (C) Effect of D-galactose on planktonic cell growth. (D) Effect of D-galactose on the biofilm formation. (E) Measurement of AI-2 production in cultures using *V. harveyi* BB170 bioassay. Relative values are presented referring the negative control (fresh AB medium). Supernatant of *V. harveyi* BB170 culture is used as positive control. Cultures incubated for 72 h are measured in each assays. In A - D, different lowercase letters represent the significant difference between AI-2-treated and non-treated sample in a group ($p < 0.05$), and different capital letters represent significant differences between the cultures with same treatment ($p < 0.05$).

3.3 Metabolomics analysis

To investigate the metabolic interactions between *L. plantarum* and *A. pasteurianus* within the biofilm, metabolomic profiling was conducted. A total of 309 metabolites were identified (Table S2). All compounds were detected in every sample, and can be used to clearly separated the sample groups in PCA (Fig. S2), consistent with the distinction by the PCA of ion profiles (Fig. S3). Among the compound classes, alcohols, amines, and ketones showed comparable levels across the three biofilm types, whereas the remaining classes differed significantly between at least two groups (Table S3). Amino acids and organic acids were the most abundant and diverse metabolites in all samples. Saccharides and their derivatives were most enriched in the *L. plantarum* mono-culture (Mo-L), followed by the *A. pasteurianus* mono-culture (Mo-A), and were lowest in the co-culture. Conversely, pyrimidines and purines were most abundant in Mo-A, intermediate in the co-culture, and least in Mo-L. Phenols were highest in Mo-A and showed comparable levels between Mo-L and the co-culture. Steroids were lowest in Mo-L and showed comparable levels between Mo-A and the co-culture.

A total of 122 significantly differential metabolites were identified between the Mo-A and the Mo-L (Fig. 3A). The variation of certain metabolites corresponded well to the known metabolic traits of the two species. For instance, *L. plantarum* produced markedly higher levels of D-phenyllactic acid and γ-aminobutyric acid (Fig. S4A), which are characteristic metabolites associated with the antifungal and functional activities[63-64]. In contrast, Mo-A exhibited elevated levels of metabolites closely linked to oxidative stress mitigation such as glutathione, oxidized glutathione, cysteinylglycine and most phenolic compounds (eg. catechol and (-)-epigallocatechin) (Fig. S4A and Table S2)[65], reflecting the strong dependence of *A. pasteurianus* on dissolved oxygen and cellular redox balance ability[66]. Furthermore, *A. pasteurianus* produced high 2-phenylethanol, a key volatile compound typically derived from yeast metabolism during vinegar fermentation[67-68].

A total of 90 differential metabolites were identified between the Mo-A and the co-culture, while 94 were detected between the Mo-L and the co-culture (Fig. 3B and C, Table S2). Forty-two metabolites were shared between the two comparisons (Fig. 3D). Among them, 30 metabolites (Fig. 3E) showed significant deviations from the expected values predicted by the simple mixture of mono-culture contents based on the relative abundances of each strain in the co-culture. These 30 metabolites were therefore considered to be markedly affected by the interspecies interactions. Of these, 16 metabolites exhibited intermediate levels between Mo-A and Mo-L, whereas 5 (cluster 2) and 9 (cluster 4) metabolites were significantly upregulated and downregulated in the co-culture, respectively. Pathway enrichment analysis of these 30 metabolites revealed substantial impacts on five KEGG pathways: purine metabolism, glycerolipid metabolism, fructose and mannose metabolism, the citrate cycle (TCA), and alanine, aspartate and glutamate metabolism (Fig. 3F). Elevated xanthine levels induce the production of reactive oxygen species via xanthine dehydrogenase, which in turn activates stress responses that upregulate the synthesis of EPS and adhesive proteins. This not only reinforces the integrity of the biofilm matrix but also enhances bacterial aggregation and surface

adhesion[69]. Accumulated 2'-deoxyadenosine can paradoxically promote QS, driving biofilm maturation[70]. Depletion of key metabolic intermediates can also elicit compensatory cellular responses that augment biofilm formation. For instance, lysine methylation of adhesins AtaA is critical for mediating adhesion in *Acinetobacter* species, and disruption of this post-translational modification (e.g., reduced N(6)-methyllysine levels) triggers excessive EPS production to stabilize biofilm aggregates[71]. These results demonstrate that co-cultivation profoundly remodels the metabolic profiles of *L. plantarum* and *A. pasteurianus, which* converge to drive increased biofilm formation.

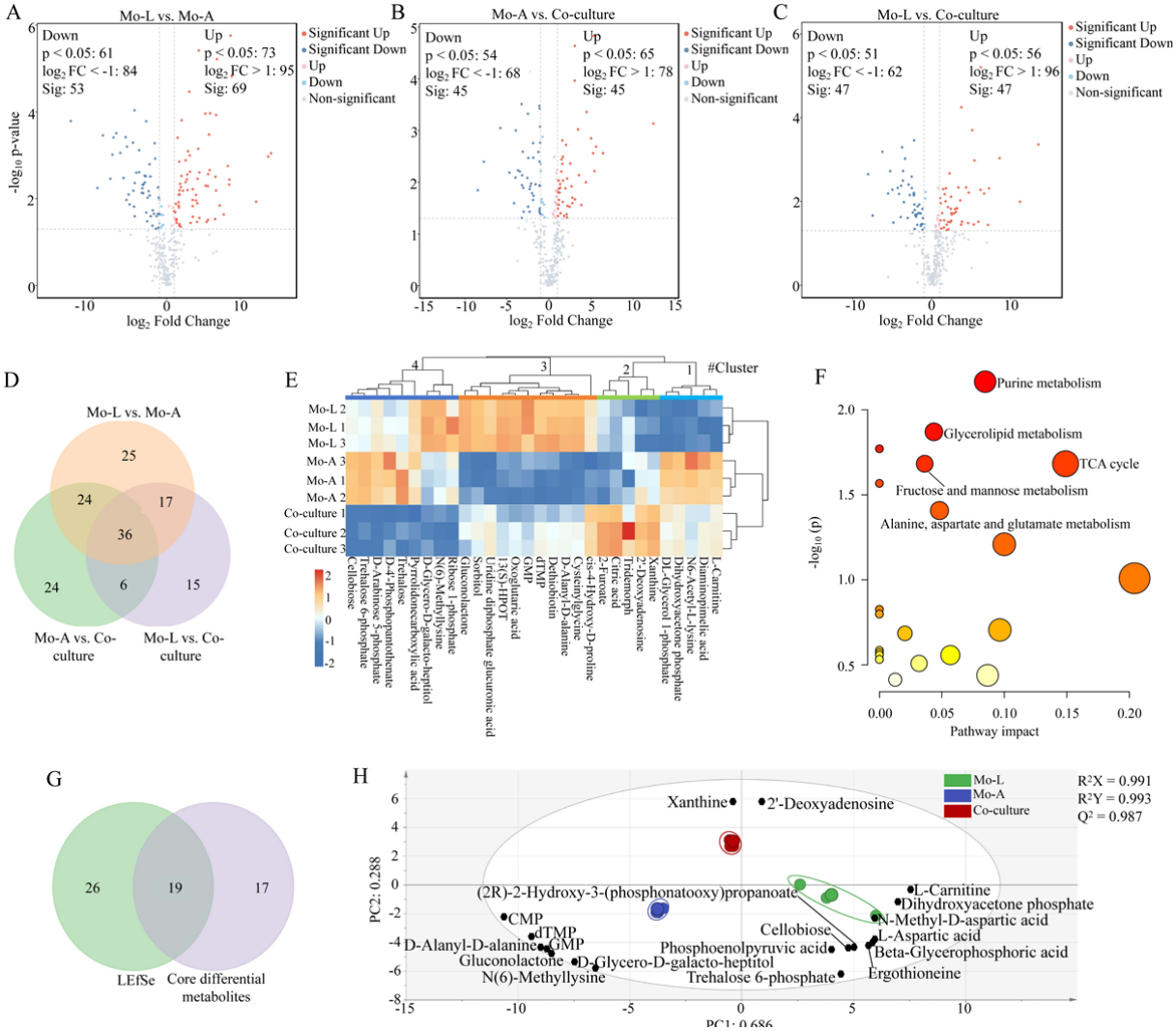


Fig. 3 Metabolomics analysis of bacterial strains embedded in biofilms. (A - C) Volcanic diagram of the differential metabolites (FDR $P < 0.05$) (A) between Mo-L and Mo-A, (B) between Mo-L and co-culture, and (C) between Mo-A and co-culture. (D) Venn diagram of differential metabolites in pairwise comparison of the 3 groups. (E) The heat maps of 30 deferential metabolites. (F) KEGG pathway analysis of the 30 metabolites. Pathways with impact factor > 0 and $P < 0.05$ are marked. (G) Venn diagram of 45 differential metabolites identified by LEfSe analysis (LDA > 2.5 and $P < 0.05$) and the 36 core ones identified in (D). (H) O_2PLS-DA biplot performed with the 19 shared differential metabolites.

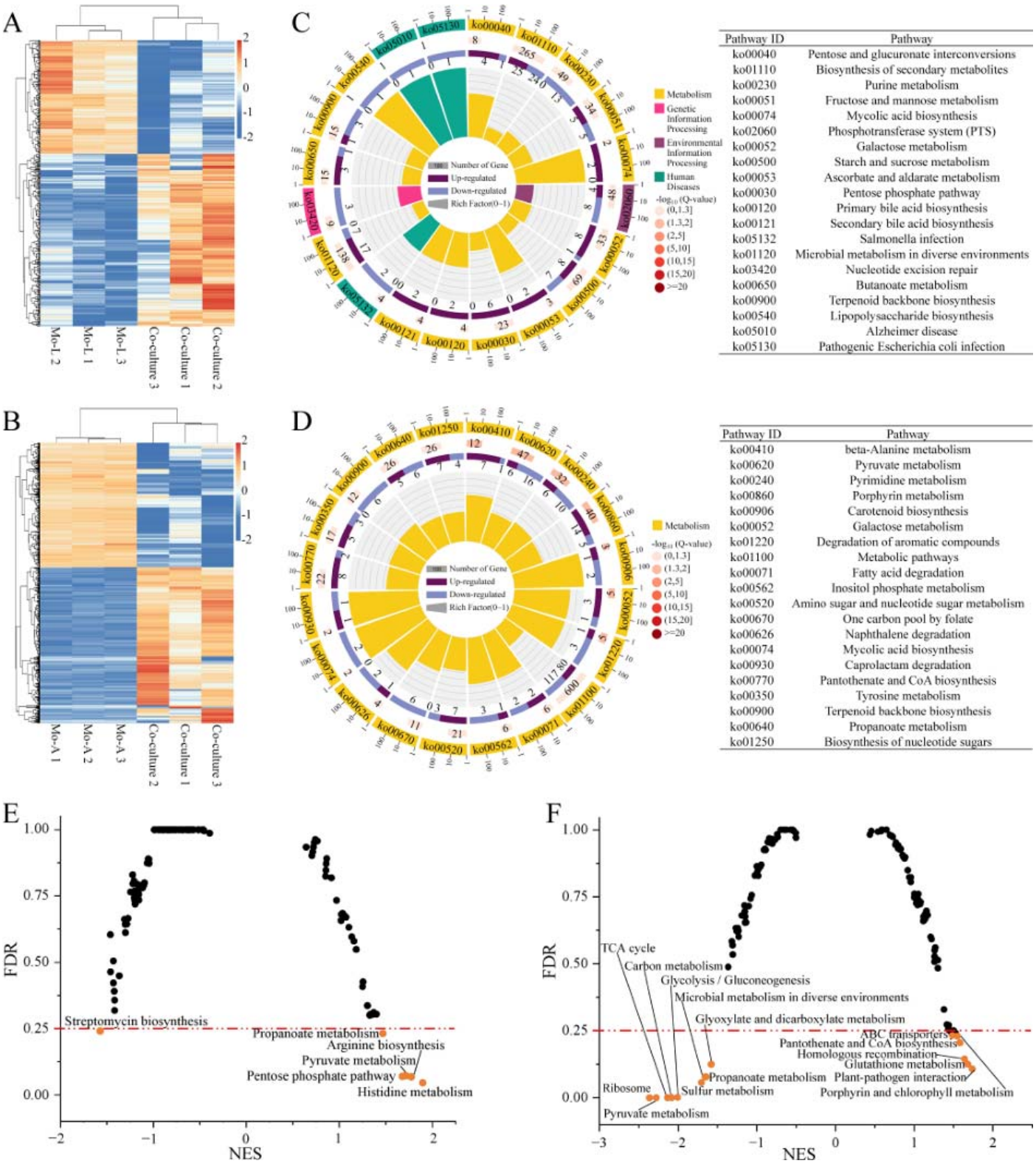
Thirty-six differential metabolites were shared among the pairwise comparisons of the three groups (Fig. 3D), and effectively distinguished the groups in PCA (Fig. S5). In the LEfSe analysis, 45 differential substances (LDA > 2.5 and $P < 0.05$) were identified as key discriminants among the groups (Fig. S6)[72]. Nineteen of these LEfSe-identified metabolites overlapped with the 36 common differential compounds (Fig. 3G). To further characterize these metabolites, O_2PLS-DA was employed with the 19 metabolites, a model

commonly used to determine the associations of characteristic metabolites with specific groups[73]. The O_2PLS-DA model, showing high explanatory and predictive performance ($R^2X = 0.991$, $R^2Y = 0.993$, $Q^2 = 0.987$), exhibited strong group separation (Fig. 3H). These compounds could therefore be considered potential biomarkers distinguishing the three cultures. The identified biomarkers highlighted distinct metabolic pathways for each culture type. Xanthine and 2'-deoxyadenosine, associated with purine metabolism, were enriched in the co-culture. Phosphoenolpyruvic acid, dihydroxyacetone phosphate, β-glycerophosphoric acid, and trehalose 6-phosphate were predominantly enriched in glycolysis pathway of Mo-L. CMP and GMP, related to pyrimidine metabolism, were enriched in Mo-A. The results highlighted the importance of enhanced purine metabolism in driving biofilm formation in the co-culture system. Beyond the effects of elevated xanthine and 2'-deoxyadenosine levels, increased metabolic flux through the purine metabolic pathway sustains the production of ATP and NADPH, thereby enhancing biofilm resilience to environmental stresses[74]. Collectively, the metabolic shifts represent a key driver of biofilm enhancement in the co-culture.

3.4 Transcriptomic analysis

A total of 26,259,476 to 94,610,044 reads were generated in transcriptomics of mono- and co-cultures of *L. plantarum* and *A. pasteurianus* (Table S4). Comparing co-cultured *L. plantarum* (Co-L) with its Mo-L identified 412 DEGs, of which 248 were upregulated and 164 downregulated in Co-L (Fig. S7A). For *A. pasteurianus*, 924 DEGs were detected in co-culture (Co-A) relative to the Mo-A, including 514 upregulated and 410 downregulated genes (Fig. S7B). HCA of the DEGs revealed a clear distinction between mono- and co-cultures (Fig. 4A and B), which was consistent with the PCA of transcriptomic profiles (Fig. S8).

In KEGG annotation, 126 and 290 DEGs were identified between Co-L and Mo-L (Table S5) and between Co-A and Mo-A (Table S6), respectively. These DEGs were largely assigned to the functional category 'Metabolism' at level 1 (Fig. 4C and D). Further, DEGs of *L. plantarum* were primarily distributed in 'ko01110 Biosynthesis of secondary metabolites' and 'ko01120 Microbial metabolism in diverse environments' (Fig. 4C). These pathways encompass multiple metabolic modules and play key roles in mediating a wide range of biological activities and microbial adaptation, including communication, competition, and interactions with the environment[75-76]. For *A. pasteurianus*, DEGs were mainly enriched in 'ko00620 Pyruvate metabolism', 'ko00240 Pyrimidine metabolism', and 'ko00860 Porphyrin metabolism' (Fig. 4D), highlighting their importance in adaptation to co-cultured biofilms. Additionally, *acpS* (holo-[acyl-carrier protein] synthase) and *fabD* ([acyl-carrier-protein] S-malonyltransferase) were enriched in the pathway of 'ko00074 Mycolic acid biosynthesis' of Co-L. Mycolic acids are the characteristic components of the cell walls of acid-fast bacteria like mycobacterial. The up-regulation of 'ko00074 Mycolic acid biosynthesis' can contribute to the mycolic acid-based permeability barrier[77-78] and biofilm formation[79]. One gene, *rfaB* (UDP-D-galactose:(glucosyl)LPS alpha-1,6-D-galactosyltransferase) involved in biosynthesis of lipopolysaccharide in bacterial cell wall, was enriched in 'ko00540 Lipopolysaccharide biosynthesis' of Co-L. The down-regulation of this pathway may also promote biofilm formation[80].



Pathway ID	Pathway
ko00040	Pentose and glucuronate interconversions
ko01110	Biosynthesis of secondary metabolites
ko00230	Purine metabolism
ko00051	Fructose and mannose metabolism
ko00074	Mycolic acid biosynthesis
ko02060	Phosphotransferase system (PTS)
ko00052	Galactose metabolism
ko00500	Starch and sucrose metabolism
ko00053	Ascorbate and aldarate metabolism
ko00030	Pentose phosphate pathway
ko00120	Primary bile acid biosynthesis
ko00121	Secondary bile acid biosynthesis
ko05132	Salmonella infection
ko01120	Microbial metabolism in diverse environments
ko03420	Nucleotide excision repair
ko00650	Butanoate metabolism
ko00900	Terpenoid backbone biosynthesis
ko00540	Lipopolysaccharide biosynthesis
ko05010	Alzheimer disease
ko05130	Pathogenic Escherichia coli infection

Pathway ID	Pathway
ko00410	beta-Alanine metabolism
ko00620	Pyruvate metabolism
ko00240	Pyrimidine metabolism
ko00860	Porphyrin metabolism
ko00906	Carotenoid biosynthesis
ko00052	Galactose metabolism
ko01220	Degradation of aromatic compounds
ko01100	Metabolic pathways
ko00071	Fatty acid degradation
ko00562	Inositol phosphate metabolism
ko00520	Amino sugar and nucleotide sugar metabolism
ko00670	One carbon pool by folate
ko00626	Naphthalene degradation
ko00074	Mycolic acid biosynthesis
ko00930	Caprolactam degradation
ko00770	Pantothenate and CoA biosynthesis
ko00350	Tyrosine metabolism
ko00900	Terpenoid backbone biosynthesis
ko00640	Propanoate metabolism
ko01250	Biosynthesis of nucleotide sugars

Fig. 4 Transcriptomics analysis of bacterial strains embedded in biofilms. (A and B) HCA of DEGs (A) between Co-L and Mo-L, and (B) between Co-A and Mo-A. (C and D) KEGG term analysis of regulated pathways (C) in Co-L compared with Mo-L, and (D) in Co-A compared with Mo-A. In C and D, the first lap indicates top 20 GO term and the number of the genes corresponds to the outer lap. The second lap indicates the number of the genes in the genome background and Q values for enrichment of the upregulated genes for the specified biological process. The third lap indicates the ratio of the upregulated genes (deep purple) and downregulated genes (light purple). The fourth lap indicates the enrichment factor of each KEGG term. (E and F) KEGG database-based GSEA analysis of regulated pathways (E) in Co-L compared with Mo-L, and (F) in Co-A compared with Mo-A. The x-axis shows the normalized enrichment score (NES), and the y-axis shows the FDR. Significantly enriched terms (FDR < 0.25) are colored by red.

GSEA further identified five upregulated pathways in Co-L compared with Mo-L, including ‘Histidine

metabolism', 'Arginine biosynthesis', 'Pyruvate metabolism', 'Pentose phosphate pathway', and 'Propanoate metabolism' (Fig. 4E and Table S7). These pathways are critical for generating molecular building blocks and energy, thereby enhancing bacterial adaptation. The expressions of various phosphotransferase transporter system (PTS) genes were increased to enhance the utilization of sugar and alcohol for pyruvate metabolism, including *scrA* (sucrose PTS), *bglF* (β-glucoside PTS), *gatA* (galactitol PTS), *gatC* (galactitol PTS), *ulaA* (L-ascorbate PTS), and *ulaC* (L-ascorbate PTS). Likewise, rhamnose utiliztion was enhanced to support pyruvate metabolism, as shown by the increased expressions of *rhaA* (rhamnose isomerase), *rhaB* (rhamnulokinase) and *rhaD* (rhamnulose-1-phosphate aldolase). The 'Pentose phosphate pathway' appeared essential for maintaining cell viability, since three genes in this pathway (*gntZ*; *gntK*; *xpk*) exhibited the highest transcriptional increases in the Co-L compared with Mo-L, accompanied by significantly elevated expression of *rbsD* (ribose/D-xylose importer). For energy supplement, *frdA* (succinate dehydrogenase flavoprotein subunit of complex II in oxidative phosphorylation pathway) was significantly upregulated, promoting ATP generation via proton translocation[81]. The upregulation of 'Arginine biosynthesis' and 'Propanoate metabolism' can contribute to enhancing acid resistance in LAB[81]. Other acid resistance mechanisms were also adopted. For instance, *ldh* (lactate dehydrogenase) was downregulated to reduce lactic acid production. All these upregulated pathways have been reported to influence biofilm formation as follows. 'Histidine metabolism' is associated with cell surface protein production[82], and is known for promoting bacterial bioflm[83]. Enhanced 'Arginine biosynthesis' has been demonstrated to promote biofilm attachment[84]. Highly active 'Pyruvate metabolism'[85], 'Pentose phosphate pathways'[86] and 'Propanoate metabolism'[87] are also reported to favor biofilm development.

Contrast to the occurrence in *L. plantarum*, carbon metabolisms (e.g. TCA cycle, Glycolysis/Gluconeogenesis, Pyruvate metabolism, Glyoxylate and dicarboxylate metabolism, and Propanoate metabolism) were repressed in Co-A compared with Mo-A (Fig. 4F and Table S8). The downregulation of 'Glyoxylate metabolism' and 'Pyruvate metabolism' has been reported in a similar study[14]. 'Sulfur metabolism', 'Ribosome' and 'Microbial metabolism in diverse environments' were also downregulated. 'Sulfur metabolism' typically cooperates with glycolysis and pyruvate metabolism to supply energy and electrons[88]. 'Ribosome' is integral to global translation processes, and represents a fundamental pathway to change basic cellular functions[89]. 'Microbial metabolism in diverse environments' reflects broad metabolic adaptation to environmental changes. Repression of these pathways likely allowed *A. pasteurianus* to avoid excess energy production, supporting survival under the low-pH, microaerobic conditions of biofilm[4,87-88]. Consistent with the metabolic repression, several nutrient intake and cell division transport genes were downregulated, including *pstA* (phosphate importer), *pstB* (phosphate importer), *cysW* (sulfate/thiosulfate importer) and *ftsX* (cell division permease). Six pathways were unregulated, including 'Plant-pathogen interaction', 'Porphyrin and chlorophyll metabolism', 'Glutathione metabolism', 'Homologous recombination', 'Pantothenate and CoA biosynthesis' and 'ABC transporters' (Fig. 4F and Table S8). Pyrroloquinoline quinine dependent alcohol dehydrogenase (PQQ-Adh)-PQQ-Aldh (aldehyde

dehydrogenase)-respiratory chain constitutes the major energy-generating system in *A. pasteurianus*[63]. Adh contains hemes c and pyrroloquinoline quinone as the prosthetic groups, and functions as the primary component of the respiratory chain[90]. Enhancement of the hemes c-related 'Porphyrin metabolism' and *adh* expression likely helped maintain homeostasis under hypoxia and acid stress[4]. Similarly, upregulated 'Glutathione metabolism', consistent with elevated glutathione and oxidized glutathione contents, provided powerful redox buffering[65]. Upregulation of 'Pantothenate and CoA biosynthesis' was associated with acid tolerance[91]. In the enriched 'Transporter' category, the upregulation of several genes, including *urtB* (urea importer), *ssuB* (alkanesulfonate importer), *btuF* (cobalamin importe) and *nasA* (nitrite importer), contributes to acid neutralization and oxidative stress mitigation[92-94]. Additional acid resistance mechanisms included upregulation of *ocd* (ornithine cyclodeaminase), *maoII* (primary-amine oxidase), and *ipdC* (indolepyruvate decarboxylase), which generate NH_3 and remove carboxyl groups to counter intracellular acidity. The expressions of genes encoding efflux pumps, such as *lagD* (lactococcin-G exporter), *lolD* (lipoprotein exporter), *lolE* (lipoprotein exporter and *lptB* (lipopolysaccharide exporter), were upregulated, resulting in the increase of components that make up of the cell envelop and biofilm[95-97]. In 'Homologous recombination', most DNA processing proteins and purinenucleoside phosphorylase have been shown the up-regulations in thicker *Streptococcus mutans* biofilms[5,98-99]. Altogether, these upregulated categories enhanced both cell survival and biofilm development.

3.5 Integrated transcriptomic and metabolomic analysis

AI-2 is formed through the cyclization of 4,5-dihydroxy-2,3-pentanedione (DPD), which is synthesized from S-adenosyl-homocysteine via two sequential enzymatic steps catalyzed by Pfs and LuxS[100]. The genes encoding Pfs, LuxS, and AI-2 receptor *LuxR* were identified in *L. plantarum,* but were absent in *A. pasteurianus*. The expressions of these three genes were unchanged in the co-culture compared with the Mo-L, which were confirmed by qRT-PCR confirming that AI-2 production was not responsible for the enhanced biofilm formation in the co-culture (Fig. S9). Moreover, no genes mapped to QS or biofilm formation pathways were significantly changed in Co-L relative to Mo-L (Fig. S10A and B). In contrast, several QS and biofilm formation genes were significantly upregulated in Co-A compared with Mo-A (Fig. S10C and D). Among these, *hfq*, a pleiotropic regulator controlling the expression of multiple genes in microbes[101], showed the highest upregulation in the Co-A transcriptome. These findings suggest that QS and biofilm-related pathways in *A. pasteurianus* may contribute to the enhancement of biofilm formation in the co-culture.

To further elucidate the regulatory mechanisms coordinating cellular responses during *L. plantarum* - *A. pasteurianus* cohabitation, a network integrating protein–metabolite interactions was constructed (Fig. 5A, Tables S9 and S10). The network encompassed 23 metabolic pathways identified through GSEA (Fig. 4E and F) and pathway enrichment of differential metabolites (Fig. 3E). The four pathways with the highest degree of connectivity were 'ko01120 Microbial metabolism in diverse environments'**,** 'ko01200 Carbon metabolism'**,** 'ko02010 ABC transporters'**, and** 'ko00230 Purine metabolism'**.** 'ko01120 Microbial metabolism in diverse environments' accounted for 5.92% (51/861) of the total associations in *A. pasteurianus* and 6.55% (22/336)

in *L. plantarum*. 'ko01200 Carbon metabolism' represented 3.25% (28/861) of edges in *A. pasteurianus* and 2.68% (9/336) in *L. plantarum*. **'ko02010 ABC transporters'** contributed 2.44% (21/861) and 4.17% (14/336), and **'ko00230 Purine metabolism'** contributed 1.97% (17/861) and 4.17% (14/336) of edges to *A. pasteurianus* and *L. plantarum*, respectively. Certain regulatory mechanisms were **strain-specific**, particularly in *A. pasteurianus*. For example, **'ko00860 Porphyrin metabolism'** was exclusively associated with *A. pasteurianus*, and numerous ribosomal genes (ko03010) showed prominent roles due to their extensive internal interactions. This highlights that while both strains share core adaptive pathways in cohabitation, *A. pasteurianus* exhibits distinctive metabolic and translational responses in the co-culture context.

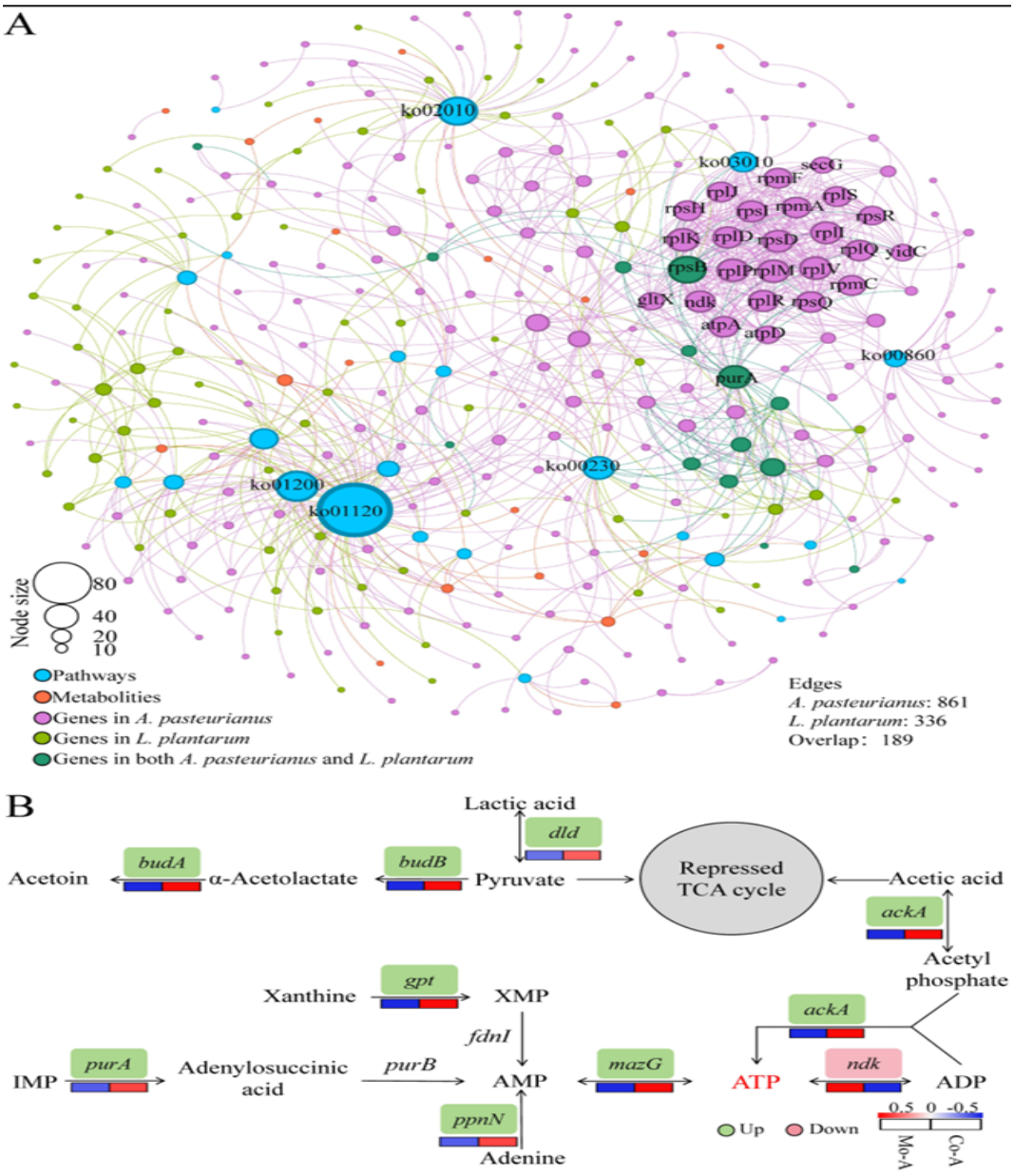


Fig. 5 Integrated transcriptomic and metabolomic analysis. (A) Interaction network of significantly differential metabolites and the associated DEGs. The 30 differential metabolites have been indicated in Fig. 4E. Metabolic pathways are available from both GSEA (21 pathways) and differential metabolites derived pathway enrichment (5 pathways). Repeated pathways are merged. Nodes represent differential metabolites, DEGs and pathways. Edges represent the associations between nodes. Key nodes are marked with the corresponding names. (B) The metabolic networks for ATP biosynthesis and lactic acid utilization in *A. pasteurianus*. The enzymatic reactions and the corresponding genes are given. Significantly regulated genes are colored.

Given the extensive associations of ***purA*** in the network, the ATP synthesis pathway was examined. In *A. pasteurianus,* except for ***ndk*** , genes closely involved in ATP production in Co-A were largely upregulated (*ackA*, *gpt*, *purA*, *ppnN*, and m*azG*) (Fig. 5B). This suggests that *A. pasteurianus* can efficiently generate ATP from exogenous molecules. Further, the upregulation of expressions of *dld* and *budB* reinforced the conversion of lactic acid into α-acetolactate in *A. pasteurianus*, wherein hydroquinone or NADH can be generated to maintain intracellular redox balance and increase ATP. Acetoin, a less toxic volatile metabolite than lactic acid, was then produced through enhanced ***budA*** under the suppressed TCA cycle[102] . These findings underscore the importance of supplemental energy and reducing power and complementary lactic acid metabolism for *A. pasteurianus* survival in co-culture. In fact, proton-motive-force-dependent efflux systems[103]and an ATP-dependent ABC transporter (AatA)[104] have been stressed the key roles to pump out acetic acid in AAB. Complementary metabolisms were also created to favor *L. plantarum in the co-culture*. For instance, sorbitol levels were higher in co-culture and Mo-A than in Mo-L (Fig. S4B), with *srlB* (sorbitol PTS) **and** *SORD* (D-glucitol:NAD+ 2-oxidoreductase) upregulated in Co-L, facilitating conversion of sorbitol into fructose via sorbose/sorbitol metabolism. As well, galactose/galactitol metabolism was complementarily constructed and beneficial to the Co-L, considering the abundant galactitol content in co-culture and Mo-A (Fig. S4B) and upregulation of most relevant DEGs in Co-L (Fig. S11). *A. pasteurianus* exhibited intense red fluorescence in CLSM images of its monocultured biofilm, indicative of severe cellular damage (Fig. 6). Such damaged cells were not detected in the co-cultured biofilm. Given that the abundance of *A. pasteurianus* was comparable between monocultured and co-cultured biofilms (Fig. 1E), metabolic crosstalk between the two strains likely represents a key mechanism underlying the enhanced survival and stress resilience of *A. pasteurianus* within the co-cultured biofilm matrix[105].

Overall, acid stress responses and complementary metabolisms were key drivers of the transcriptomic and metabolomic adaptations of *L. plantarum* and *A. pasteurianus* in co-cultured biofilms. Notably, energy generation and intracellular redox balance were emphasized in *A. pasteurianus*, whereas the provision of biomass building blocks was prominent in *L. plantarum*. These adaptive changes facilitated a symbiotic relationship that favored *A. pasteurianus*, and comprehensively elucidated the observation that biofilm formation in the co-culture exceeded that of either mono-culture.

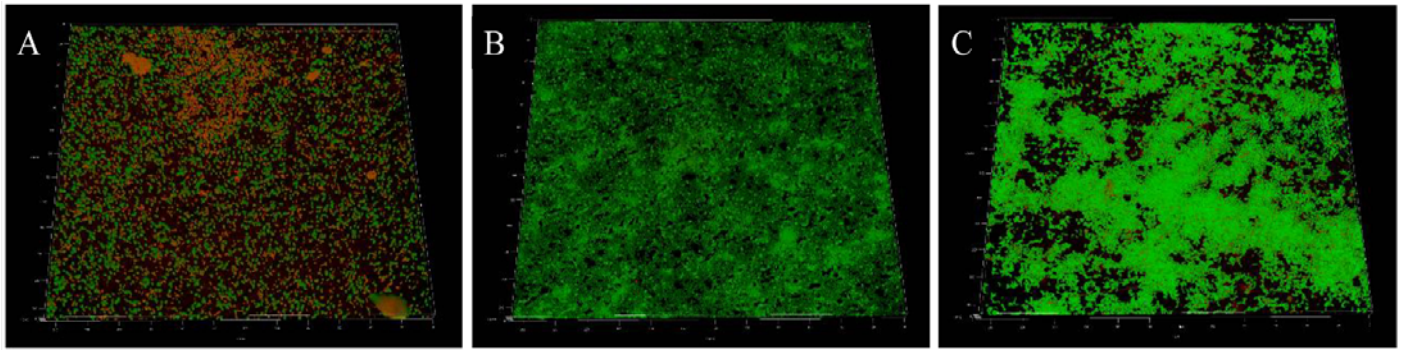


Fig. 6 CLSM images of biofilms in (A) mono-culture of *A. pasteurianus*, (B) mono-culture of *L. plantarum*, and co-culture of *A. pasteurianus* and *L. plantarum.*

3.6 Effect of A. pasteurianus-L. plantarum *co-culture* on vinegar production

We further investigated the effects of *A. pasteurianus-L. plantarum* co-fermentation on the physicochemical properties of vinegar. Acetic acid produced by AAB is the most critical quality of vinegar. LAB are also major contributors to organic acid biosynthesis, with lactic acid being the second most abundant organic acid in the product[51]. LAB fermentation not only imparts unique flavors, but its product lactic acid also plays an important role in mitigating the pungency of acetic acid. The two organic acids have been proved to be important secondary carbon source for various bacteria. Consistent with expectations, the contents of total acids and lactic acid were significantly higher in the *A. pasteurianus-L. plantarum* co-fermentation compared with the *A. pasteurianus* monoculture (Fig. 7A). Notably, acetic acid content was also elevated in the co-fermentation (Fig. 7A), which could be explained by the enhanced cellular *and* Adh gene expression of *A. pasteurianus*. A*s well, L. plantarum can* preferentially produce acetic acid[106]. Furthermore, the contents of other organic acids (oxalic acid, tartaric acid, malic acid, citric acid and succinic acid) were significantly increased in the co-fermentation, which may result from the upregulated carbon metabolism of *L. plantarum* (Fig. 7A).

TP and TF are the primary contributors to the antioxidant activity of vinegar, a property recognized as a key health-promoting characteristic of vinegar[107]. The contents of TP and TF, as well as DPPH and ABTS radical scavenging activities, were all significantly increased in vinegar produced by *A. pasteurianus-L. plantarum* co-fermentation (Fig. 7B and C). A previous study demonstrated that these antioxidant-characteristics were markedly enhanced by LAB fermentation, which were greatly correlated with the enrichment of pyruvate metabolism, glycolysis/gluconeogenesis and fructose and mannose metabolism as described in our study[108]. Collectively, these findings suggest that *A. pasteurianus-L. plantarum* co-fermentation holds great potential for industrial application to improve the physicochemical and functional properties of vinegar.

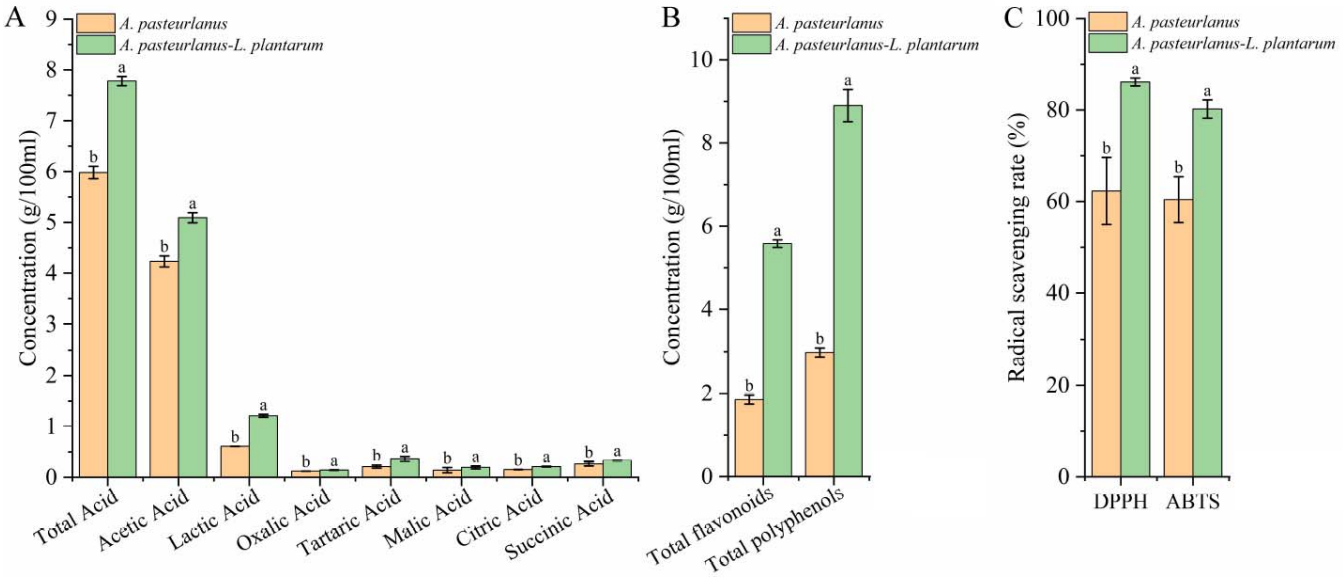


Fig. 7 Effects of *L. plantarum-A. pasteurianus* co-fermentation on (A) organic acids, (B) TP and TF contents, and (C) DPPH and ABTS radical-scavenging activities of vinegar.

4. Conclusions

A. pasteurianus showed enhanced growth in bicultures with *L. casei*, *L. plantarum*, and *L. fermentum*. Notably, biofilm formation was markedly elevated in the *L. plantarum-A. pasteurianus* co-culture. Metabolomic analysis revealed extensive metabolic pathway perturbations in the in the *L. plantarum-A. pasteurianus* co-cultured biofilm compared with monocultured biofilms. Transcriptomic data further delineated the regulatory mechanisms of bacterial adaptive responses. Beyond acid neutralization, *L. plantarum* primarily upregulated pathways for molecular building block biosynthesis, while *A. pasteurianus* reinforced energy supply and intracellular redox homeostasis. Complementary pathways, including lactic acid, sorbose/sorbitol, and galactose/galactitol metabolism, were also critical for interspecific interaction. Enhanced biosynthesis and export of lipopolysaccharides, lipoproteins, organic acids, amino acids, and nucleotides, and upregulated quorum sensing and biofilm formation pathways in *A. pasteurianus*, collectively drove robust co-cultured biofilm formation. Furthermore, *A. pasteurianus-L. plantarum* co-fermentation significantly improved the vinegar characteristics of acid production capacity and antioxidant activity. This study elucidates the regulatory mechanisms of bacterial adaption and biofilm formation in the *L. plantarum-A. pasteurianus* co-culture, providing valuable insights for industrial vinegar fermentation applications.

Competing interests

The authors declare no competing interests.

Acknowledgements

This work was supported by National Natural Science Foundation of China (32272299) and Hubei Province Central Guiding Local Science and Technology Development Special Project (2024ELA005).

References

[1] Sutherland, I. W., Hughes, K. A., Skillman, L. C., & Tait, K. (2004). The interaction of phage and biofilms. FEMS Microbiol Lett, 232(1), 1-6. https://doi.org/10.1016/s0378-1097(04)00041-2

[2] Wang, Y., Bian, Z., & Wang, Y. (2022). Biofilm formation and inhibition mediated by bacterial quorum sensing. Appl Microbiol Biotechnol, 106(19-20), 6365-6381. https://doi.org/10.1007/s00253-022-12150-3

[3] Ng, W. L., & Bassler, B. L. (2009). Bacterial quorum-sensing network architectures. Annu Rev Genet, 43, 197-222. https://doi.org/10.1146/annurev-genet-102108-134304

[4] Jia, K., Wang, G., Liang, L., Wang, M., Wang, H., & Xu, X. (2017). Preliminary transcriptome analysis of mature biofilm and planktonic cells of *Salmonella Enteritidis* exposure to acid stress. Front Microbiol, 8, 1861. https://doi.org/10.3389/fmicb.2017.01861

[5] Jiang, S., Huang, X., Zhang, C., Cai, Z., & Zou, T. (2015). Morphological and proteomic analyses of the biofilms generated by *Streptococcus mutans* isolated from caries-active and caries-free adults. Journal of Dental Sciences, 10. https://doi.org/10.1016/j.jds.2014.09.001

[6] Costerton, J. W., Lewandowski, Z., Caldwell, D. E., Korber, D. R., & Lappin-Scott, H. M. (1995). Microbial biofilms. Annual Review of Microbiology, 49:711-745. https://doi.org/10.1146/ANNUREV.MI.49.100195.003431

[7] Stoodley, P., Sauer, K., Davies, D. G., & Costerton, J. W. (2002). Biofilms as complex differentiated communities. Annu Rev Microbiol, 56, 187-209. https://doi.org/10.1146/annurev.micro.56.012302.160705

[8] Trachoo, N., & Brooks, J. D. (2005). Attachment and heat resistance of *Campylobacter jejuni* on *Enterococcus faecium* Biofilm. Pakistan Journal of Biological Sciences, 8(4), 599-605. https://doi.org/10.3923/pjbs.2005.599.605

[9] Mosteller, T. M., & Bishop, J. R. (1993). Sanitizer efficacy against attached bacteria in a milk biofilm. J Food Prot, 56(1), 34-41. https://doi.org/10.4315/0362-028x-56.1.34

[10] Olanbiwoninu, A. A., & Odunfa, S. A. (2018). Microbial interaction in selected fermented vegetable condiments in Nigeria. International Food Research Journal, 25(1), 439-445. https://api.semanticscholar.org/CorpusID:199385936

[11] Winters, M., Arneborg, N., Appels, R., & Howell, K. (2019). Can community-based signalling behaviour in *Saccharomyces cerevisiae* be called quorum sensing? A critical review of the literature. FEMS Yeast Res, 19(5). https://doi.org/10.1093/femsyr/foz046

Nie, Z., Zheng, Y., Xie, S., Zhang, X., Song, J., Xia, M., & Wang, M. (2017). Unraveling the correlation between microbiota succession and metabolite changes in traditional Shanxi aged vinegar. Sci Rep, 7(1), 9240. https://doi.org/10.1038/s41598-017-09850-6

Moens, F., Lefeber, T., & De Vuyst, L. (2014). Oxidation of metabolites highlights the microbial interactions and role of *Acetobacter pasteurianu*s during cocoa bean fermentation. Appl Environ Microbiol, 80(6), 1848-1857. https://doi.org/10.1128/aem.03344-13

Xia, M., Zhang, X., Xiao, Y., Sheng, Q., Tu, L., Chen, F., Yan, Y., Zheng, Y., & Wang, M. (2022). Interaction of acetic acid bacteria and lactic acid bacteria in multispecies solid-state fermentation of traditional Chinese cereal vinegar. Front Microbiol, 13, 964855. https://doi.org/10.3389/fmicb.2022.964855

[15] Aoudia, N., Rieu, A., Briandet, R., Deschamps, J., Chluba, J., Jego, G., Garrido, C., & Guzzo, J. (2016). Biofilms of *Lactobacillus plantarum* and *Lactobacillus fermentum*: Effect on stress responses, antagonistic effects on pathogen growth and immunomodulatory properties. Food Microbiol, 53(Pt A), 51-59. https://doi.org/10.1016/j.fm.2015.04.009

[16] Mgomi, F. C., Yang, Y. R., Cheng, G., & Yang, Z. Q. (2023). Lactic acid bacteria biofilms and their antimicrobial potential against pathogenic microorganisms. Biofilm, 5, 100118. https://doi.org/10.1016/j.bioflm.2023.100118

[17] Cui, Y., Wang, D., Zhang, L., & Qu, X. (2025). Research progress on the regulatory mechanism of biofilm formation in probiotic lactic acid bacteria. Crit Rev Food Sci Nutr, 65(25), 4869-4883. https://doi.org/10.1080/10408398.2024.2400593

[18] Sun, L. L., Zhang, Y., Guo, X. J., Zhang, L. D., Zhang, W., Man, C. X., & Jiang, Y. J. (2020). Characterization and transcriptomic basis of biofilm formation by *Lactobacillus plantarum* J26 isolated from traditional fermented dairy products. Lwt-Food Science and Technology, 125, 109333. https://doi.org/10.1016/j.lwt.2020.109333

[19] Furukawa, S., Watanabe, T., Toyama, H., & Morinaga, Y. (2013). Significance of microbial symbiotic coexistence in traditional fermentation. J Biosci Bioeng, 116(5), 533-539. https://doi.org/10.1016/j.jbiosc.2013.05.017

[20] Furukawa, S., Yoshida, K., Ogihara, H., Yamasaki, M., & Morinaga, Y. (2010). Mixed-species biofilm formation by direct cell-cell contact between brewing yeasts and lactic acid bacteria. Biosci Biotechnol Biochem, 74(11), 2316-2319. https://doi.org/10.1271/bbb.100350

[21] Furukawa, S., Nojima, N., Yoshida, K., Hirayama, S., Ogihara, H., & Morinaga, Y. (2011). The importance of inter-species cell-cell co-aggregation between *Lactobacillus plantarum* ML11-11 and *Saccharomyces cerevisiae* BY4741 in mixed-species biofilm formation. Biosci Biotechnol Biochem, 75(8), 1430-1434. https://doi.org/10.1271/bbb.100817

[22] Liang, J., Wang, Y., Wang, T., Chu, C., Yi, J., & Liu, Z. (2025). Enhancing fermented vegetable flavor with *Lactobacillus plantarum* and *Rhodotorula mucilaginosa*. Food Res Int, 200, 115500. https://doi.org/10.1016/j.foodres.2024.115500

[23] Pannella, G., Lombardi, S. J., Coppola, F., Vergalito, F., Iorizzo, M., Succi, M., Tremonte, P., Iannini, C., Sorrentino, E., & Coppola, R. (2020). Effect of Biofilm Formation by *Lactobacillus plantarum* on the Malolactic Fermentation in Model Wine. Foods, 9(6). https://doi.org/10.3390/foods9060797

[24] Hu, Q., Qi, Y., Liu, C., Chen, Q., Mai, X., Zhu, Z., & Ma, B. (2024). Effects of *Lactobacillus plantarum* cofermentation on the flavor and taste characteristics of mango vinegar. Journal of Food Measurement and Characterization, 18(5), 3744-3756. https://doi.org/10.1007/s11694-024-02446-5

[25] Qiang, X., Zhao, M., Xia, T., Wang, Q., Yu, J., Qiao, C., Zhang, H., Lv, S., Liu, Y., & Wang, M. (2025). Effect of Different Fermentation Methods on the Physicochemical, Bioactive and Volatile Characteristics of Wolfberry Vinegar. Foods, 14(6). https://doi.org/10.3390/foods14061078

[26] Wan, N., Wang, M., Wang, L., & Wang, D. (2026). Improvement of the quality and flavor profiles of persimmon vinegar by bioaugmented inoculation with Lactobacillus acidophilus, *Lactiplantibacillus plantarum* and *Wickerhamomyces anomalus*. Food Chem X, 35, 103725. https://doi.org/10.1016/j.fochx.2026.103725

[27] Xu, S., Qi, W., Xie, Y., Cheng, J., & Ban, Q. (2026). Improvement of starch fine structure, physicochemical properties and digestive characteristics of adlay seeds by fermentation with *Lactobacillus plantarum* and *Lactobacillus paracasei*. International Journal of Biological Macromolecules, 151547. https://doi.org/10.1016/j.ijbiomac.2026.151547

[28] Zhang, M., Li, X., Mu, D., Cai, J., Zhang, M., Liu, Y., Zheng, Z., Jiang, S., & Wu, X. (2022). Co-fermentation metabolism characteristics of apple vinegar with *Acetobacter pasteurianus* and *Lactobacillus plantarum*. Journal of Food Processing and Preservation, 46(7), e16605. https://doi.org/10.1111/jfpp.16605

[29] Bassler, B. L., Greenberg, E. P., & Stevens, A. M. (1997). Cross-species induction of luminescence in the quorum-sensing bacterium Vibrio harveyi. J Bacteriol, 179(12), 4043-4045. https://doi.org/10.1128/jb.179.12.4043-4045.1997

[30] Gómez, N. C., Ramiro, J. M., Quecan, B. X., & de Melo Franco, B. D. (2016). Use of potential probiotic lactic Acid bacteria (LAB) biofilms for the control of L*isteria monocytogenes*, *Salmonella typhimurium*, and *Escherichia coli* O157:H7 biofilms formation. Front Microbiol, 7, 863. https://doi.org/10.3389/fmicb.2016.00863

[31] Stepanovic, S., Vukovic, D., Dakic, I., Savic, B., & Svabic-Vlahovic, M. (2000). A modified microtiter-plate test for quantification of staphylococcal biofilm formation. J Microbiol Methods, 40(2), 175-179. https://doi.org/10.1016/s0167-7012(00)00122-6

[32] Benomar, S., Ranava, D., Cárdenas, M. L., Trably, E., Rafrafi, Y., Ducret, A., Hamelin, J., Lojou, E., Steyer, J. P., & Giudici-Orticoni, M. T. (2015). Nutritional stress induces exchange of cell material and energetic coupling between bacterial species. Nat Commun, 6, 6283. https://doi.org/10.1038/ncomms7283

[33] Bassler, B. L., Wright, M., Showalter, R. E., & Silverman, M. R. (1993). Intercellular signalling in *Vibrio harveyi*: sequence and function of genes regulating expression of luminescence. Mol Microbiol, 9(4), 773-786. https://doi.org/10.1111/j.1365-2958.1993.tb01737.x

[34] Ryu, E. J., Sim, J., Sim, J., Lee, J., & Choi, B. K. (2016). D-Galactose as an autoinducer 2 inhibitor to control the biofilm formation of periodontopathogens. J Microbiol, 54(9), 632-637. https://doi.org/10.1007/s12275-016-6345-8

[35] Smith, C. A., Want, E. J., O'Maille, G., Abagyan, R., & Siuzdak, G. (2006). XCMS: processing mass spectrometry data for metabolite profiling using nonlinear peak alignment, matching, and identification. Anal Chem, 78(3), 779-787. https://doi.org/10.1021/ac051437y

[36] Wishart, D. S., Tzur, D., Knox, C., Eisner, R., Guo, A. C., Young, N., Cheng, D., Jewell, K., Arndt, D., Sawhney, S., Fung, C., Nikolai, L., Lewis, M., Coutouly, M. A., Forsythe, I., Tang, P., Shrivastava, S., Jeroncic, K., Stothard, P., Querengesser, L. (2007). HMDB: the human metabolome database. Nucleic Acids Res, 35(Database issue), D521-526. https://doi.org/10.1093/nar/gkl923

[37] Horai, H., Arita, M., Kanaya, S., Nihei, Y., Ikeda, T., Suwa, K., Ojima, Y., Tanaka, K., Tanaka, S., Aoshima, K., Oda, Y., Kakazu, Y., Kusano, M., Tohge, T., Matsuda, F., Sawada, Y., Hirai, M. Y., Nakanishi, H., Ikeda, K., Nishioka, T. (2010). MassBank: a public repository for sharing mass spectral data for life sciences. J Mass Spectrom, 45(7), 703-714. https://doi.org/10.1002/jms.1777

[38] Sud, M., Fahy, E., Cotter, D., Brown, A., Dennis, E. A., Glass, C. K., Merrill, A. H., Jr., Murphy, R. C., Raetz, C. R., Russell, D. W., & Subramaniam, S. (2007). LMSD: LIPID MAPS structure database. Nucleic Acids Res, 35(Database issue), D527-532. https://doi.org/10.1093/nar/gkl838

[39] Abdelrazig, S., Safo, L., Rance, G. A., Fay, M. W., Theodosiou, E., Topham, P. D., Kim, D. H., & Fernández-Castané, A. (2020). Metabolic characterisation of *Magnetospirillum gryphiswaldense* MSR-1 using LC-MS-based metabolite profiling. RSC Adv, 10(54), 32548-32560. https://doi.org/10.1039/d0ra05326k

[40] Ogata, H., Goto, S., Sato, K., Fujibuchi, W., Bono, H., & Kanehisa, M. (1999). KEGG: Kyoto Encyclopedia of Genes and Genomes. Nucleic Acids Res, 27(1), 29-34. https://doi.org/10.1093/nar/27.1.29

[41] Gagnebin, Y., Tonoli, D., Lescuyer, P., Ponte, B., de Seigneux, S., Martin, P. Y., Schappler, J., Boccard, J., & Rudaz, S. (2017). Metabolomic analysis of urine samples by UHPLC-QTOF-MS: Impact of normalization strategies. Anal Chim Acta, 955, 27-35. https://doi.org/10.1016/j.aca.2016.12.029

[42] Martin, M. (2011). Cutadapt removes adapter sequences from high-throughput sequencing reads. EMBnet.journal, 17(1), 10-12. https://doi.org/10.14806/ej.17.1.200

[43] Kim, D., Paggi, J. M., Park, C., Bennett, C., & Salzberg, S. L. (2019). Graph-based genome alignment and genotyping with HISAT2 and HISAT-genotype. Nat Biotechnol, 37(8), 907-915. https://doi.org/10.1038/s41587-019-0201-4

[44] Wang, B., Shao, Y., Chen, T., Chen, W., & Chen, F. (2015). Global insights into acetic acid resistance mechanisms and genetic stability of *Acetobacter pasteurianus* strains by comparative genomics. Sci Rep, 5, 18330. https://doi.org/10.1038/srep18330

[45] Anders, S., Pyl, P. T., & Huber, W. (2015). HTSeq--a Python framework to work with high-throughput sequencing data. Bioinformatics, 31(2), 166-169. https://doi.org/10.1093/bioinformatics/btu638

[46] Xia, J., & Wishart, D. S. (2011). Web-based inference of biological patterns, functions and pathways from metabolomic data using MetaboAnalyst. Nat Protoc, 6(6), 743-760. https://doi.org/10.1038/nprot.2011.319

[47] Subramanian, A., Tamayo, P., Mootha, V. K., Mukherjee, S., Ebert, B. L., Gillette, M. A., Paulovich, A., Pomeroy, S. L., Golub, T. R., Lander, E. S., & Mesirov, J. P. (2005). Gene set enrichment analysis: a knowledge-based approach for interpreting genome-wide expression profiles. Proc Natl Acad Sci U S A, 102(43), 15545-15550. https://doi.org/10.1073/pnas.0506580102

[48] Zhou, G., Soufan, O., Ewald, J., Hancock, R. E. W., Basu, N., & Xia, J. (2019). NetworkAnalyst 3.0: a visual analytics platform for comprehensive gene expression profiling and meta-analysis. Nucleic Acids Res, 47(1), 234-241. https://doi.org/10.1093/nar/gkz240

[49] Bastian, M., Heymann, S., & Jacomy, M. (2009). Gephi: an open source software for exploring and manipulating networks. Proceedings of the International AAAI Conference on Web and Social Media, 3(1), 361-362. https://doi.org/10.1609/icwsm.v3i1.13937

[50] Liu, Z., Wang, C., Chen, H., Ren, X., Li, W., Xu, N., Zhang, Y., Wang, J., & Hu, Y. (2022). Effect of changing the melanoidins by decoction on the release of volatiles in Zhenjiang aromatic vinegar. Food Res Int, 158, 111453. https://doi.org/10.1016/j.foodres.2022.111453

[51] Hu, Y., Zheng, C., Chen, H., Wang, C., Ren, X., Fu, S., Xu, N., Li, P., Song, J., & Wang, C. (2023). Characteristics and discrimination of the commercial chinese Four Famous Vinegars based on flavor compositions. Foods, 12(9), 1865. https://doi.org/10.3390/foods12091865

[52] Wang, Y., Hong, X., Liu, J., Zhu, J., & Chen, J. (2020). Interactions between fish isolates *Pseudomonas fluorescens* and *Staphylococcus aureus* in dual-species biofilms and sensitivity to carvacrol. Food Microbiol, 91, 103506. https://doi.org/10.1016/j.fm.2020.103506

[53] Yang, H., Yu, Y., Fu, C., & Chen, F. (2019). Bacterial acid resistance toward organic weak acid revealed by RNA-Seq transcriptomic analysis in *Acetobacter pasteurianus*. Front Microbiol, 10, 1616. https://doi.org/10.3389/fmicb.2019.01616

[54] Fernández, A., Alvarez-Ordóñez, A., López, M., & Bernardo, A. (2009). Effects of organic acids on thermal inactivation of acid and cold stressed *Enterococcus faecium*. Food Microbiol, 26(5), 497-503. https://doi.org/10.1016/j.fm.2009.03.002

[55] Luttik, M., Van Spanning, R., Schipper, D., Van Dijken, J. P., & Pronk, J. T. (1997). The low biomass yields of the acetic acid bacterium *Acetobacter pasteurianus* are due to a low stoichiometry of respiration-coupled proton translocation. Appl Environ Microbiol, 63(9), 3345-3351. https://doi.org/10.1128/aem.63.9.3345-3351.1997

[56] Zheng, Y., Zhang, R., Yin, H., Bai, X., Chang, Y., Xia, M., & Wang, M. (2017). *Acetobacter pasteurianus* metabolic change induced by initial acetic acid to adapt to acetic acid fermentation conditions. Appl Microbiol Biotechnol, 101(18), 7007-7016. https://doi.org/10.1007/s00253-017-8453-8

[57] Chai, L. J., Qiu, T., Lu, Z. M., Deng, Y. J., Zhang, X. J., Shi, J. S., & Xu, Z. H. (2020). Modulating microbiota metabolism via bioaugmentation with *Lactobacillus casei* and *Acetobacter pasteurianus* to enhance acetoin accumulation during cereal vinegar fermentation. Food Res Int, 138(Pt A), 109737. https://doi.org/10.1016/j.foodres.2020.109737

[58] Federle, M. J., & Bassler, B. L. (2003). Interspecies communication in bacteria. The Journal of clinical investigation, 112(9), 1291-1299. https://doi.org/10.1172/jc1200320195

[59] Kaper, J. B., & Sperandio, V. (2005). Bacterial cell-to-cell signaling in the gastrointestinal tract. Infect Immun, 73(6), 3197-3209. https://doi.org/10.1128/iai.73.6.3197-3209.2005

[60] Li, B., Gu, Y., Yan, C. L., Jia, Y. B., & He, Y. F. (2016). Screening and identification of AI-2 high-producing lactic acid bacteria. Food Sci Technol, 37, 185-188. https://doi.org/10.13386/j.issn1002-0306.2016.02.029

[61] Yoshida, A., & Kuramitsu, H. K. (2002). Multiple *Streptococcus mutans* genes are involved in biofilm formation. Appl Environ Microbiol, 68(12), 6283-6291. https://doi.org/10.1128/aem.68.12.6283-6291.2002

[62] Nobile, C. J., Fox, E. P., Nett, J. E., Sorrells, T. R., Mitrovich, Q. M., Hernday, A. D., Tuch, B. B., Andes, D. R., & Johnson, A. D. (2012). A recently evolved transcriptional network controls biofilm development in *Candida albicans*. Cell, 148(1-2), 126-138. https://doi.org/10.1016/j.cell.2011.10.048

[63] Lavermicocca, P., Valerio, F., Evidente, A., Lazzaroni, S., Corsetti, A., & Gobbetti, M. (2000). Purification and characterization of novel antifungal compounds from the sourdough *Lactobacillus plantarum* strain 21B. Appl Environ Microbiol, 66(9), 4084-4090. https://doi.org/10.1128/aem.66.9.4084-4090.2000

[64] Li, H., & Cao, Y. (2010). Lactic acid bacterial cell factories for gamma-aminobutyric acid. Amino Acids, 39(5), 1107-1116. https://doi.org/10.1007/s00726-010-0582-7

[65] Smirnova, G. V., & Oktyabrsky, O. N. (2005). Glutathione in bacteria. Biochemistry (Mosc), 70(11), 1199-1211. https://doi.org/10.1007/s10541-005-0248-3

[66] Edwardson, C. F., & Hollibaugh, J. T. (2018). Composition and activity of microbial communities along the redox gradient of an alkaline, hypersaline, lake. Front Microbiol, 9, 14. https://doi.org/10.3389/fmicb.2018.00014

[67] Мамєєва, О. Г., Остапчук, А. М., & Підгорський, В. С. (2010). The 2-phenylethanol and ethanol production by yeast *Saccharomyces cerevisiae*. Mìkrobìologìâ ì Bìotehnologìâ, 0(1), 14-22. https://doi.org/10.18524/2307-4663.2010.1(9).98318

[68] Garavaglia, J., Flôres, S. H., Pizzolato, T. M., Peralba, M. d., & Ayub, M. A. (2007). Bioconversion of l -phenylalanine into 2-phenylethanol by *Kluyveromyces marxianus* in grape must cultures. World Journal of Microbiology and Biotechnology, 23(9), 1273-1279. https://doi.org/10.1007/s11274-007-9361-3

[69] Srivastava, M., Mallard, C., Barke, T., Hancock, L. E., & Self, W. T. (2011). A selenium-dependent xanthine dehydrogenase triggers biofilm proliferation in *Enterococcus faecalis* through oxidant production. Journal of bacteriology, 193(7), 1643–1652. https://doi.org/10.1128/JB.01063-10

[70] Mirghani, R., Saba, T., Khaliq, H., Mitchell, J., Do, L., Chambi, L., Diaz, K., Kennedy, T., Alkassab, K., Huynh, T., Elmi, M., Martinez, J., Sawan, S., & Rijal, G. (2022). Biofilms: Formation, drug resistance and alternatives to conventional approaches. AIMS microbiology, 8(3), 239-277. https://doi.org/10.3934/microbiol.2022019

[71] Inoue, S., Yoshimoto, S., & Hori, K. (2025). A new target of multiple lysine methylation in bacteria. Journal of Bacteriology, 207(1), e00325-24. https://doi:10.1101/2024.05.15.594293.

[72] Moreno-Arrones, O. M., Serrano-Villar, S., Perez-Brocal, V., Saceda-Corralo, D., Morales-Raya, C., Rodrigues-Barata, R., Moya, A., Jaen-Olasolo, P., & Vano-Galvan, S. (2020). Analysis of the gut microbiota in alopecia areata: identification of bacterial biomarkers. J Eur Acad Dermatol Venereol, 34(2), 400-405. https://doi.org/10.1111/jdv.15885

[73] Carraro, S., Giordano, G., Reniero, F., Carpi, D., Stocchero, M., Sterk, P. J., & Baraldi, E. (2013). Asthma severity in childhood and metabolomic profiling of breath condensate. Allergy, 68(1), 110-117. https://doi.org/10.1111/all.12063

[74] Guillín, Y., Ortiz, C. , & Hidalgo, W. (2025). Comparative metabolic study of planktonic and sessile cells in salmonella enteritidis atcc 13076: elucidating metabolic pathways driving biofilm formation. PLOS ONE, 20(1), p.e0317420 1932-6203. https://doi.org/10.1371/journal.pone.0317420

[75] Hibbing, M. E., Fuqua, C., Parsek, M. R., & Peterson, S. B. (2010). Bacterial competition: surviving and thriving in the microbial jungle. Nat Rev Microbiol, 8(1), 15-25. https://doi.org/10.1038/nrmicro2259

[76] Charlop-Powers, Z., Owen, J. G., Reddy, B. V., Ternei, M. A., & Brady, S. F. (2014). Chemical-biogeographic survey of secondary metabolism in soil. Proc Natl Acad Sci U S A, 111(10), 3757-3762. https://doi.org/10.1073/pnas.1318021111

[77] Lee, R. E., Armour, J. W., Takayama, K., Brennan, P. J., & Besra, G. S. (1997). Mycolic acid biosynthesis: definition and targeting of the Claisen condensation step. Biochim Biophys Acta, 1346(3), 275-284. https://doi.org/10.1016/s0005-2760(97)00051-9

[78] Colston, M. J., & Lamb, F. I. (1989). Molecular biology of the *Mycobacteria*. Leprosy review, 60(2), 89-93. https://doi.org/10.5935/0305-7518.19890011

[79] Pacheco, S. A., Hsu, F. F., Powers, K. M., & Purdy, G. E. (2013). MmpL11 protein transports mycolic acid-containing lipids to the *Mycobacterial* cell wall and contributes to biofilm formation in *Mycobacterium smegmatis*. J Biol Chem, 288(33), 24213-24222. https://doi.org/10.1074/jbc.M113.473371

[80] BROOKE, J. S., VO, A., & WATTS, P. (2008). Mutation of a lipopolysaccharide synthesis gene results in increased biofilm of *Stenotrophomonas maltophilia* on plastic and glass surfaces. Annals of Microbiology, 8(1), 35-40. https://doi.org/10.1007/bf03179442

[81] Wang, C., Cui, Y., & Qu, X. (2018). Mechanisms and improvement of acid resistance in lactic acid bacteria. Arch Microbiol, 200(2), 195-201. https://doi.org/10.1007/s00203-017-1446-2

[82] Cabral, M. P., Soares, N. C., Aranda, J., Parreira, J. R., Rumbo, C., Poza, M., Valle, J., Calamia, V., Lasa, I., & Bou, G. (2011). Proteomic and functional analyses reveal a unique lifestyle for *Acinetobacter baumannii* biofilms and a key role for histidine metabolism. J Proteome Res, 10(8), 3399-3417. https://doi.org/10.1021/pr101299j

[83] Rébora, K., Laloo, B., & Daignan-Fornier, B. (2005). Revisiting purine-histidine cross-pathway regulation in *Saccharomyces cerevisiae*: a central role for a small molecule. Genetics, 170(1), 61-70. https://doi.org/10.1534/genetics.104.039396

[84] Tada, A., Nakayama-Imaohji, H., Yamasaki, H., Hasibul, K., Yoneda, S., Uchida, K., Nariya, H., Suzuki, M., Miyake, M., & Kuwahara, T. (2016). Cleansing effect of acidic L-arginine on human oral biofilm. BMC Oral Health, 16, 40. https://doi.org/10.1186/s12903-016-0194-z

[85] Resch, A., Leicht, S., Saric, M., Pásztor, L., Jakob, A., Götz, F., & Nordheim, A. (2006). Comparative proteome analysis of *Staphylococcus aureus* biofilm and planktonic cells and correlation with transcriptome profiling. Proteomics, 6(6), 1867-1877. https://doi.org/10.1002/pmic.200500531

[86] Zhou, Q., Feng, X., Zhang, Q., Feng, F., Yin, X., Shang, J., Qu, H., & Luo, Q. (2012). Carbon catabolite control is important for *Listeria monocytogenes* biofilm formation in response to nutrient availability. Curr Microbiol, 65(1), 35-43. https://doi.org/10.1007/s00284-012-0125-4

[87] Sun, C., Zhao, X., Jiao, Z., Peng, J., Zhou, L., Yang, L., Huang, M., Tian, C., & Guo, G. (2022). The antimicrobial peptide AMP-17 derived from *Musca domestica* inhibits biofilm formation and eradicates mature biofilm in *Candida albicans*. Antibiotics (Basel), 11(11), 1474. https://doi.org/10.3390/antibiotics11111474

[88] Zheng, X., Wang, Y. Z., Wu, J., Wu, Y., Long, M., & Chen, Y. G. (2024). Enhanced degradation of methanethiol via operational pH regulation in biofilm reactor: Insight of sulfur metabolism pathways and microbial adaptation mechanism. Chemical Engineering Journal, 495, 153414. https://doi.org/10.1016/j.cej.2024.153414

[89] Starosta, A. L., Lassak, J., Jung, K., & Wilson, D. N. (2014). The bacterial translation stress response. FEMS Microbiol Rev, 38(6), 1172-1201. https://doi.org/10.1111/1574-6976.12083

[90] Matsushita, K., Yakushi, T., Toyama, H., Shinagawa, E., & Adachi, O. (1996). Function of multiple heme c moieties in intramolecular electron transport and ubiquinone reduction in the quinohemoprotein alcohol dehydrogenase-cytochrome c complex of *Gluconobacter suboxydans*. J Biol Chem, 271(9), 4850-4857. https://doi.org/10.1074/jbc.271.9.4850

[91] Rojony, R., Martin, M., Campeau, A., Wozniak, J. M., Gonzalez, D. J., Jaiswal, P., Danelishvili, L., & Bermudez, L. E. (2019). Quantitative analysis of *Mycobacterium avium subsp. hominissuis* proteome in response to antibiotics and during exposure to different environmental conditions. Clin Proteomics, 16, 39. https://doi.org/10.1186/s12014-019-9260-2

[92] Liu, Y., Tang, H., Lin, Z., & Xu, P. (2015). Mechanisms of acid tolerance in bacteria and prospects in biotechnology and bioremediation. Biotechnol Adv, 33(7), 1484-1492. https://doi.org/10.1016/j.biotechadv.2015.06.001

[93] Van Der Ploeg, J. R., Cummings, N. J., Leisinger, T., & Connerton, I. F. (1998). *Bacillus subtilis* genes for the utilization of sulfur from aliphatic sulfonates. Microbiology (Reading), 144 (9), 2555-2561. https://doi.org/10.1099/00221287-144-9-2555

[94] Birch, C. S., Brasch, N. E., McCaddon, A., & Williams, J. H. (2009). A novel role for vitamin B(12): Cobalamins are intracellular antioxidants in vitro. Free Radic Biol Med, 47(2), 184-188. https://doi.org/10.1016/j.freeradbiomed.2009.04.023

[95] Kibler, K., Svetz, J., Nguyen, T. L., Shaw, C., & Shaulsky, G. (2003). A cell-adhesion pathway regulates intercellular communication during *Dictyostelium* development. Dev Biol, 264(2), 506-521. https://doi.org/10.1016/j.ydbio.2003.08.025

[96] Miyamoto, A., Matsuyama, S., & Tokuda, H. (2002). Dominant negative mutant of a lipoprotein-specific molecular chaperone, LolA, tightly associates with LolCDE. FEBS Lett, 528(1-3), 193-196. https://doi.org/10.1016/s0014-5793(02)03305-7

[97] Sperandeo, P., Cescutti, R., Villa, R., Di Benedetto, C., Candia, D., Dehò, G., & Polissi, A. (2007). Characterization of lptA and lptB, two essential genes implicated in lipopolysaccharide transport to the outer membrane of *Escherichia coli*. J Bacteriol, 189(1), 244-253. https://doi.org/10.1128/jb.01126-06

[98] Rathsam, C., Eaton, R. E., Simpson, C. L., Browne, G. V., Berg, T., Harty, D. W. S., & Jacques, N. A. (2005). Up-regulation of competence- but not stress-responsive proteins accompanies an altered metabolic phenotype in *Streptococcus mutans* biofilms. Microbiology, 151(Pt 6), 1823-1837. https://doi.org/10.1099/mic.0.27830-0

[99] Rathsam, C., Eaton, R. E., Simpson, C. L., Browne, G. V., Valova, V. A., Harty, D. W., & Jacques, N. A. (2005). Two-dimensional fluorescence difference gel electrophoretic analysis of *Streptococcus mutans* biofilms. J Proteome Res, 4(6), 2161-2173. https://doi.org/10.1021/pr0502471

[100] Sun, J., Daniel, R., Wagner-Döbler, I., & Zeng, A. P. (2004). Is autoinducer-2 a universal signal for interspecies communication: a comparative genomic and phylogenetic analysis of the synthesis and signal transduction pathways. BMC Evol Biol, 4, 36. https://doi.org/10.1186/1471-2148-4-36

[101] Lenz, D. H., Mok, K. C., Lilley, B. N., Kulkarni, R. V., Wingreen, N. S., & Bassler, B. L. (2004). The small RNA chaperone Hfq and multiple small RNAs control quorum sensing in *Vibrio harveyi* and *Vibrio cholerae*. Cell, 118(1), 69-82. https://doi.org/10.1016/j.cell.2004.06.009

[102] Adler, P., Frey, L. J., Berger, A., Bolten, C. J., Hansen, C. E., & Wittmann, C. (2014). The key to acetate: metabolic fluxes of acetic acid bacteria under cocoa pulp fermentation-simulating conditions. Appl Environ Microbiol, 80(15), 4702-4716. https://doi.org/10.1128/aem.01048-14

[103] Matsushita, K., Inoue, T., Adachi, O., & Toyama, H. (2005). *Acetobacter aceti* possesses a proton motive force-dependent efflux system for acetic acid. J Bacteriol, 187(13), 4346-4352. https://doi.org/10.1128/jb.187.13.4346-4352.2005

[104] Nakano, S., Fukaya, M., & Horinouchi, S. (2006). Putative ABC transporter responsible for acetic acid resistance in *Acetobacter aceti*. Appl Environ Microbiol, 72(1), 497-505. https://doi.org/10.1128/aem.72.1.497-505.2006

[105] Zhang, Y., Cai, Y., Zhang, B., & Zhang, Y. P. J. (2024). Spatially structured exchange of metabolites enhances bacterial survival and resilience in biofilms. Nat Commun, 15(1), 7575. https://doi.org/10.1038/s41467-024-51940-3

[106] De Marco, I., Oliveira de Moraes, J., Nunes Ferreira, F., Turnes Pasini Deolindo, C., Eller Pazzini, I. A., da Silva Vale, A., Verruck, S., & De Dea Lindner, J. (2025). Production of type III sourdough by spray- and freeze-drying focusing on organic acids, volatile organic compounds, and cell viability during storage. ACS Food Science & Technology, 5(1), 292-305. https://doi.org/10.1021/acsfoodscitech.4c00826

[107] Xie, X., Zheng, Y., Liu, X., Cheng, C., Zhang, X., Xia, T., Yu, S., & Wang M. (2017). Antioxidant activity of Chinese Shanxi aged vinegar and its correlation with polyphenols and flavonoids during the brewing process. Journal of Food Science, 82(10), 2479-2486. https://doi.org/10.1111/1750-3841.13914

[108] Hou, F. , Cai, Y. , & Wang, J. (2023). Antioxidant capacity changes and untargeted metabolite profile of broccoli during lactic acid bacteria fermentation. Fermentation-basel, 9(5), 474. https://10.3390/fermentation9050474